Environmental Impact Assessment Review 116 (2026) 108110

Contents lists available at ScienceDirect

Environmental Impact Assessment Review

journal homepage: www.elsevier.com/locate/eiar

Optimizing reactive maintenance intervals for the sustainable rehabilitation of chloride-exposed coastal buildings with MMC-based concrete structure

Antonio J. Sánchez-Garrido [a,*], Ignacio J. Navarro [a], Víctor Yepes [b]

[a] Dept. of Construction Engineering, Universitat Politècnica de València, 46022 Valencia, Spain
[b] Institute of Concrete Science and Technology (ICITECH), Universitat Politècnica de València, 46022 Valencia, Spain

ARTICLE INFO

Keywords:
Sustainable design
Life cycle assessment
Social impacts
Reactive maintenance
Chloride exposure
Reinforced concrete
Decision support systems
Building rehabilitation

ABSTRACT

Coastal cities face significant challenges in maintaining their infrastructure due to harsh environmental conditions, such as high humidity and airborne chlorides, which accelerate material degradation. This issue is particularly critical for reinforced concrete structures in beachfront buildings, such as hotels, where corrosion is a common and progressive problem. Timely maintenance and repair are essential to prevent structural failures caused by accidental loads, such as wind or earthquakes, which can compromise safety. Historically, the focus in construction has been on reducing environmental impact, often overlooking the importance of maintenance and end-of-life stages. This paper presents a novel, integrated methodology combining preventive design assessment with reactive maintenance optimization to study the sustainability of repair strategies for maintenance in coastal cities of buildings with reinforced concrete exposed to chloride-induced corrosion. The study focuses on structures based on Modern Methods of Construction (MMC) to minimize life cycle impact by optimizing material consumption compared to traditional construction. Twelve preventive design alternatives are evaluated, each subjected to four maintenance strategies addressing different damage levels caused by deterioration throughout the structure's service life. A FUCOM-TOPSIS model aggregates eight sustainability criteria—economic costs, life-cycle environmental burdens, and social performance indicators—to identify optimal year-by-year maintenance intervals and rank alternatives. Results reveal that the most sustainable designs involve multiresistant cement, hydrophobic anti-corrosion impregnation, and silica fume additive, achieving sustainability ratings up to 86 % higher than the baseline. This approach enhances the resilience and sustainability of coastal infrastructure, effectively addressing challenges posed by harsh environmental conditions and supporting long-term, sustainable urban development.

1. Introduction

The construction sector is the most extensive industry globally, accounting for 13 % of the world's GDP and 39 % of energy-related CO_2 emissions (McKinsey and Company, 2023). In Europe, buildings consume 40 % of energy and produce 36 % of emissions. The EU targets net-zero carbon buildings by 2030 and climate neutrality by 2050 through stricter regulations and a circular economy to curb this. Cement alone accounts for 10 % of global emissions (Lehne and Preston, 2018), highlighting the need for urgent action.

The Sustainable Development Goals (SDGs) promote conservation to reduce structures' environmental impact. Effective maintenance enhances performance, efficiency, and durability, especially in harsh environments. Durability—key to modern regulations—extends a structure's lifespan by preventing deterioration. Research highlights the benefits of predicting wear (Frangopol et al., 2017) and optimizing maintenance (Ait-Ali et al., 2024; Han and Frangopol, 2022) for safety and cost efficiency. Reinforcing or rehabilitating existing structures is more economically and environmentally sustainable than rebuilding them (Alba-Rodríguez et al., 2017). Preventive maintenance—based on scheduled inspections and interventions—minimizes damage progression and resource consumption, enhancing structural lifespan (Navarro et al., 2019). Meanwhile, reactive maintenance addresses failures after occurrence but often entails higher costs and extended downtime

* Corresponding author.
E-mail addresses: ajsangar@doctor.upv.es (A.J. Sánchez-Garrido), ignamar1@cam.upv.es (I.J. Navarro), vyepesp@cst.upv.es (V. Yepes).

https://doi.org/10.1016/j.eiar.2025.108110
Received 19 March 2025; Received in revised form 28 July 2025; Accepted 31 July 2025
Available online 15 August 2025

(Stenström et al., 2016). Integrating both within a multi-objective life-cycle framework improves resilience by balancing costs, risks, and sustainability over the infrastructure's lifetime (Yang and Frangopol, 2019).

Building on the importance of maintenance strategies, consideration of environmental factors further reduces infrastructure's footprint. Advances include CO_2 reduction in road maintenance (Choi, 2019), AI-driven optimization of prestressed slab bridges (Yepes-Bellver et al., 2024) or three-dimensional dynamic models of thermomechanical optimization for bridge maintenance (Zhou et al., 2024). Life cycle analysis evaluates buildings (Sharma et al., 2012), Ultra High-Performance Concrete (Di Summa et al., 2023), and railway prestressed concrete sleepers (Del Serrone et al., 2025). Predictive models aid concrete bridge redesign in coastal areas (Hadizadeh-Bazaz et al., 2023).

Modern Methods of Construction (MMC) are innovative, process-oriented techniques that incorporate prefabrication, off-site manufacturing, and digital design tools. These methods aim to improve construction efficiency, quality, and environmental performance. MMC significantly contributes to sustainability by optimizing material use, reducing resource consumption, and accelerating project timelines (Sánchez-Garrido et al., 2023). In contrast to traditional systems, MMC adopts circular economy principles to minimize waste (Schöggl et al., 2020), promote the reuse of components, and integrate recycled materials, thereby enhancing both environmental and economic outcomes (Ding et al., 2025).

The SDGs emphasize social factors in infrastructure, yet assessments often focus on aesthetics, user impact, and worker safety while overlooking economic growth, service access, and job creation (UNEP/SETAC, 2013). No universal method exists for measuring social lifecycle impacts, but research explores their assessment (Josa and Borrion, 2025) and maintenance optimization (Navarro et al., 2018). Public institutions now prioritize sustainable infrastructure, enforcing stricter environmental and social standards, promoting responsible material use, and supporting certifications like ENVISION, BREEAM, and LEED (Ascione et al., 2022).

Construction has long prioritized initial impact over long-term maintenance, causing premature deterioration (Zhang et al., 2017; Rincon et al., 2024). Key threats include carbonation, chloride corrosion, sulfate attack, and freeze-thaw cycles, often worsened by water-borne contaminants. Codes regulate cement content, water/cement ratio, and reinforcement coverage. Durability improvements involve optimized concrete mixes (Sánchez-Garrido et al., 2024b), protective coatings, reinforced steel, electrochemical treatments, and high-strength repair materials.

Corrosion is common in exposed reinforced concrete (RC) structural elements (Rodrigues et al., 2021), weakening steel reinforcement and compromising integrity over time (Hu et al., 2022). While reinforced concrete is durable, prolonged exposure—especially in coastal areas (Patrisia et al., 2022)—can cause cracking, spalling, and deterioration, increasing vulnerability to fires, hurricanes, floods, and earthquakes (Bru et al., 2018). This shortens a structure's lifespan, poses safety risks, and leads to costly repairs (Bastidas-Arteaga and Schoefs, 2015). Strengthening existing structures and effective maintenance, particularly in harsh environments, is crucial for sustainability (Wittocx et al., 2022).

Focusing on cost, environmental impact, or social effects alone is insufficient. Budget-conscious maintenance ensures profitability, low-impact practices conserve resources, and well-maintained infrastructure improves safety and reliability (Nolan et al., 2021). A balanced approach integrating these factors is key to resilient infrastructure. However, sustainability trade-offs require multi-criteria decision-making (MCDM) (Zavadskas et al., 2016), where weighted factors guide optimal solutions (Zhu et al., 2021). Recent reviews have highlighted the importance of MCDM methods in evaluating sustainable retrofitting strategies for buildings and infrastructure (Villalba et al., 2024). In particular, hybrid approaches that combine neutrosophic logic-based group AHP to handle uncertainty with classical MCDM methods such as TOPSIS have demonstrated strong performance in modeling sustainability under complex conditions, for example, in chloride-induced degradation scenarios affecting bridge decks (Navarro et al., 2020).

This study's key innovation lies in integrating a year-by-year life-cycle assessment with a hybrid FUCOM–TOPSIS model to evaluate twelve preventive structural designs and four reactive maintenance strategies tailored to varying damage levels in chloride-exposed MMC-based reinforced concrete structures. While FUCOM (Haqbin, 2022) and TOPSIS (Madanchian and Taherdoost, 2023) have been individually applied in civil engineering, their combined use as a hybrid model provides a novel, structured, and consistency-driven framework for multi-criteria prioritization. The model incorporates expert knowledge to assess alternatives across eight carefully selected criteria covering economic costs, life-cycle environmental burdens, and social performance indicators. This hybridization strengthens the robustness of trade-off analyses among conflicting sustainability objectives, aligning weight assignment and alternative ranking with expert judgment and system behavior. As a result, the proposed approach effectively bridges early design configurations with long-term maintenance scheduling, offering a comprehensive and scalable tool for sustainable infrastructure planning in aggressive coastal environments.

2. Study components and methodology

2.1. Sustainable performance evaluation of building structures in harsh conditions

Sustainability in structural design requires environmental, social, and economic analysis. Environmental assessments follow ISO 14040 and 14044 (ISO, 2006a, 2006b), while social life cycle frameworks stem from UNEP/SETAC (2009). Compliance ensures consistency through four steps: defining goals, conducting inventory analysis, selecting methods, and presenting results. Economic analysis is performed through life cycle cost assessment (LCCA), which quantifies all relevant costs—including initial construction costs and future maintenance costs—over the structure's service life. While construction costs occur at the initial time and are not discounted, future maintenance costs are discounted to present value following guidelines from ISO 15686-5 (ISO, 2017).

2.1.1. Establishing objectives and defining the scope

This study evaluates a dozen design alternatives to enhance concrete durability in marine environments, comparing them to a reference hotel building in Sancti Petri (Chiclana de la Frontera, Cádiz). The baseline design (BAS) features a three-story guest room module with a gravel-covered maintenance-accessible roof. Its substructure consists of a mat foundation, while the superstructure includes three biaxial voided flat slabs (Fig. 1) built on-site using MMC (Sánchez-Garrido et al., 2024a). This system incorporates high-density, 100 % recycled polyethylene void formers (Fig. 2), known as "UNIDOME" slabs (Schnellenbach-Held and Pfeffer, 2002). This approach improves efficiency by reducing self-weight, enabling greater spans and higher load-bearing capacity than conventional designs (Alhassan et al., 2022).

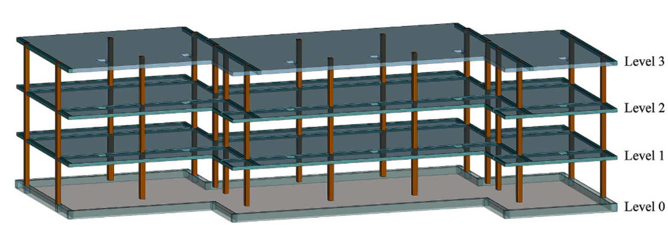

Fig. 1. 3D visualization of the baseline (BAS) structure.

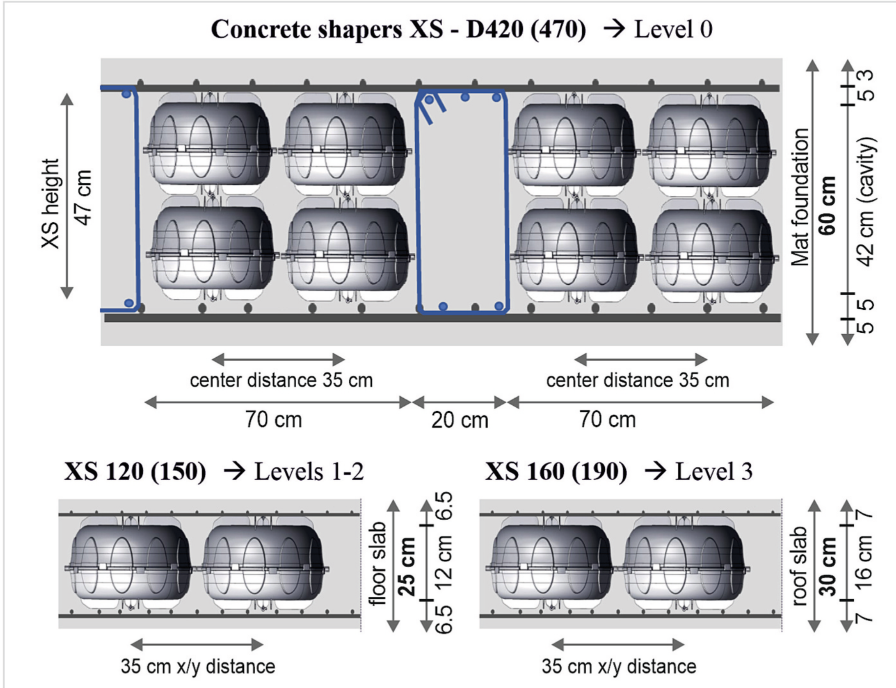

Fig. 2. "Unidome" multi-axial voided slab system.

This study explores preventive measures to enhance concrete resistance to chloride penetration and corrosion, extending its service life. The first three options incorporate 5 % silica fume (SF5) or 10–20 % fly ash (FA10/FA20) by cement weight, improving strength, durability, and workability while reducing permeability and heat of hydration. However, limited local availability and high transportation costs make these additives less practical. A more feasible alternative is sulfate-resistant cement (SRC), widely used in the region for durability in harsh conditions. Lowering the water-to-binder ratio (WCR) from 0.60 to 0.50 also enhances concrete density and reduces porosity.

This study explores durability enhancements for reinforced concrete. Increasing reinforcement cover from 25 to 30 mm to 45 mm (CR45) improves protection while oversizing concrete and steel by 25 % (ODSE) boosts rigidity, durability, and safety under extreme conditions. Surface treatments, such as hydrophobic impregnation with corrosion inhibitors (ACHI), help block chloride ingress. Additionally, cathodic protection (CCPR) is proposed, applying a 10 mm cement mortar coating with silica sand and additives to encase a titanium mesh anode, with power supply cables placed every 1.5 m.

Finally, concrete structures subjected to chlorides can achieve more excellent durability by replacing carbon steel reinforcement with corrosion-resistant alternatives like galvanized steel (GALV), which has a protective zinc coating, or stainless steel (INOX), whose chromium-rich composition offers superior corrosion resistance, reducing maintenance and extending the structure's lifespan.

For the maintenance phase, three repair strategies are proposed, each adapted to the extent of damage over time as determined by the deterioration model outlined in Section 3. These strategies are as follows: (1) replacement of the protective coating, a standard step applied in all cases; (2) cleaning, repair, and passivation of the oxidized reinforcement; and (3) replacement or strengthening of the partially corroded reinforcement. Repair interventions focus exclusively on exposed concrete elements: the undersides of cantilever slabs at levels 1, 2 (25 cm thick), and 3 (30 cm thick), as well as the perimeter edges of slabs on balconies and facades. These components face harsh marine conditions that accelerate chloride ingress and reinforcement corrosion. As the only concrete surfaces exposed and protected only by minimal coatings—such as thin render or paint—they are especially vulnerable to deterioration. The repair scope also includes beams at the edges of cantilevered balconies, the most exposed elements showing early signs of degradation, initially through corrosion of the stirrups. Conversely, interior beams behind the facade and columns embedded within the double-leaf brick wall with an air cavity and thermal insulation benefit from effective protection against environmental aggressors. This preserves their structural integrity, limiting maintenance to routine preventive measures without requiring repairs.

This study follows ISO 14040 standards, using a consistent functional unit for life cycle assessments. It evaluates economic, environmental, and social impacts per square meter of the foundation and affected structure, totaling 2132 m^2 over a 100-year lifespan. To ensure a realistic analysis, a service life twice the standard set by national regulations is considered (Ministry of Transport, Mobility and Urban Agenda, 2021). A "gate-to-grave" approach assesses impacts from construction through maintenance to decommissioning.

2.1.2. *Impact assessment*

A collection of eight criteria is developed to evaluate the sustainability of various design solutions, focusing on the three key dimensions: economical, environmental, and social. In the economic dimension, two criteria are considered. The first criterion (C1) accounts for the construction costs of the functional unit for each design alternative, including material and machinery costs. The second criterion (C2) considers long-term maintenance costs for each design. To accurately reflect the value of future expenses, maintenance costs incurred during the use phase are discounted to present value using a social discount rate. This discounting approach is consistent with the guidelines of ISO 15686-5 (ISO, 2017), which standardizes life cycle costing procedures in construction, ensuring appropriate treatment of future maintenance costs. This rate is essential in cost-benefit analyses, especially for public infrastructure projects with extended lifespans and significant social impacts. For this study, a discount rate of 2 % (d = 2 %) is applied, following recommendations from recent literature on sustainability and infrastructure economics (Schoenmaker and Schramade, 2024).

This rate balances the ethical consideration of valuing future costs nearly as much as present ones while maintaining economic practicality. Boardman et al. (2018) support using this discount rate in their comprehensive review, highlighting its suitability for long-term public investments. A higher discount rate would reduce the importance of future maintenance costs, potentially leading to underinvestment in durability and sustainability measures. In contrast, a lower rate might overstate distant benefits, reducing feasibility. Therefore, the selected 2 % rate provides a prudent and balanced approach for evaluating life cycle costs in coastal infrastructure rehabilitation under climate uncertainties. Maintenance costs are discounted according to Eq. 1:

$$LCC = \sum_{t=t_0}^{t_{SL}} C_i \times 1 \Big/ (1+d)^{t-t_0} \tag{1}$$

where LCC denotes the total Life Cycle Cost of the structure, C_i denotes the maintenance costs at time t, t_0 is the start of the evaluation period, t_{SL} indicates the projected duration, and d represents the rate applied for discounting.

The second group of criteria emphasizes on the environmental sphere of sustainability. Criteria C3 and C4 measure the environmental impacts of each alternative's construction and maintenance phases. These criteria evaluate the consequences of producing building materials and the activities involved in construction and the reactive maintenance. Both environmental criteria are evaluated using the ReCiPe 2016 methodology (Huijbregts et al., 2017). This procedure converts emissions from material and energy flows into 18 midpoint impact categories, reflecting their effect on the environment. These categories include global warming potential, eutrophication, and water use. The ReCiPe methodology then aggregates these midpoint categories into three endpoint indicators, quantifying the damage to human well-being, ecosystems, and resource supply. These endpoint indicators are normalized and combined into a single final indicator, representing the overall environmental impact of the evaluated system. Sánchez-Garrido et al. (2024b) provides a more in-depth explanation of the environmental assessment methodology.

The final four criteria assess the social impacts of constructing and maintaining each design alternative. These impacts are evaluated using the framework of Sánchez-Garrido et al. (2021), adapted to this study. The first stage consists of identifying stakeholders affected by the structure (UNEP/SETAC, 2009). This methodology, which uses indicators, focuses on three principal groups in Spanish building construction: workers, users, and the local community. Stakeholder identification is conducted through a hotspot analysis (UNEP/SETAC, 2013), which is aligned with the hotel's regional development plan in Cádiz, Spain. Negative impacts on consumers and workers are assessed over the building's lifespan, considering construction and repair durations. Reducing these durations is crucial, as they directly affect pedestrian and resident safety while also minimizing accident risks for workers. Additionally, externalities such as noise and vibrations impact the local community.

The first two social criteria, C5 and C6, assess each design's constructability and ease of maintenance, respectively. These factors are crucial for sustainability, as more extended construction or maintenance times lead to more significant externalities, intensifying negative impacts on the local community and its users. C5 and C6 are evaluated based on the equivalent performance of construction and maintenance activities, considering their simultaneity. To estimate this equivalent performance, we adopt a formulation adapted from Sánchez-Garrido et al. (2021), grounded in the simultaneity model proposed by Valderrama (2009). Valderrama highlights that construction duration estimates must consider the average number of activities occurring simultaneously, as assuming sequential execution results in unrealistic project timelines. Specifically, the average number of simultaneous activities can be approximated by the square root of the total number of activities in the project. This reflects that larger projects allow more concurrent operations, but the relationship is sublinear, preventing overestimation of concurrency and thus unrealistic productivity loss. The proposed formulation is as follows:

$$P_{EL} = \frac{\sum T_m \bullet \sqrt{m_0} + \sum T_w \bullet \sqrt{a_0}}{m_0 + a_0} \tag{2}$$

where P_{EL} is the equipment and labor productivity in hours, based on an 8-h workday, 5 days per week, and 22 working days per month, T_m is the time (hours) for each piece of equipment or machinery, and T_w is the time (hours) for each construction worker, m_o is the count of activities involving machinery, and a_o is the quantity of activities involving workers. The simultaneity factor, represented by the square root (SQRT) of m_o and a_o, accounts for overlapping activities that affect productivity. Up to two simultaneous activities are excluded from interference calculations, as these do not significantly impact productivity in this construction context. This methodology balances accuracy and simplicity, allowing for more realistic estimations of constructability and maintenance efforts without requiring detailed scheduling data. This metric converts total labor and machinery hours into productivity-adjusted execution time, accounting for concurrency of activities. Lower equivalent performance values indicate shorter, more efficient processes, with fewer disruptions to workers, users, and surrounding communities.

The last two social criteria, C7 and C8, measure the employment generated by construction and maintenance activities. This positive social impact is quantified regarding total working hours required, including labor and machinery use (Navarro et al., 2018).

Sustainability is evaluated based on these eight impact categories. Since the criteria often conflict, The TOPSIS method (Hwang and Yoon, 1981) is applied to decision-making. The Full Consistency Method (FUCOM) (Haqbin, 2022) is utilized to establish each criterion's relevance. FUCOM is a MCDM technique that prioritizes criteria while maintaining consistency and reducing the number of comparisons. Compared to the widely used Analytic Hierarchy Process (AHP), FUCOM offers a more straightforward and faster approach with explicit consistency enforcement. The FUCOM method follows these steps:

Step 1: Identify the set of criteria (C_1, C_2, … C_n) that are crucial to the decision-making dilemma.

Step 2: Rank the criteria in descending order of importance based on the judgments of the decision-maker.

Step 3: Compare adjacent criteria in the ranking to establish their relative importance ratios $k_{i,i+1}$, where $k_{i,i+1}$ represents how many times more important C_i is compared to C_{i+1}.

Step 4: Considering the relative importance ratios $k_{i,i+1}$, the weight of each criterion can be expressed as a function of one single criterion, usually the least important one. For example:

$$w_1 = k_{1,2} \bullet k_{2,3} \bullet \ldots \bullet k_{(n-1)n} \bullet w_n \tag{3}$$

Step5: To check consistency, it shall be verified that the derived importance ratios k_{ij} between non-adjacent criteria are aligned with the initial judgments. For example

$$w_i \big/ w_{i+2} = w_{i,i+1} \bullet w_{i+1,i+2}$$

Then, the deviation Δ_k between the derived and expected ratios is obtained as:

$$\Delta_k = \left| \frac{w_i / w_j}{\prod k_{x,x+1}} - 1 \right| \tag{4}$$

If Δ_k exceeds a previously established threshold, pairwise comparisons need to be readjusted until consistency is reached. If $\Delta_k = 0$, full consistency is achieved.

Step 6: Once acceptable consistency has been achieved, normalize the resulting weights so that their sum equals 1:

$$w_i^{normalized} = \frac{w_i}{\sum_{j=1}^{n} w_i} \tag{5}$$

The resulting normalized weights represent the relative importance of each criterion and can now be used for evaluating alternatives.

After defining criteria weights, TOPSIS is used to identify the design alternative and maintenance interval that maximize life cycle sustainability. First, it selects the most sustainable maintenance interval for each design by evaluating impacts across eight criteria weighted using FUCOM. Once optimal intervals are set, TOPSIS determines the most sustainable of the 12 design alternatives. Fig. 3 outlines the study's framework, methodology, and sequential stages.

2.1.3. Inventory analysis

By ISO 14040 standards for life cycle assessment, accurate data is essential to assess a project's economic, environmental, and social impacts. This study uses reliable sources to ensure dependable results. Economic data is obtained from official Spanish construction databases, like CYPE Ingenieros (2025), and supplemented with supplier information for a more detailed cost analysis. The costs include materials, labor, equipment, machinery, and other direct construction expenses. Detailed tables have been included in the appendix to enhance clarity and address comparative analysis needs. Table A.1 provides unit costs and effectively characterizes the different building alternatives, while Table A.2 outlines the costs associated with reactive maintenance strategies. These comprehensive tables support a clear and structured comparison of all alternatives within the life cycle cost assessment framework.

Inventory data was sourced from the Ecoinvent 3.2 database for the environmental assessment. Table 1 lists material flows for each preventive design during construction, while Table 2 details flows for reactive maintenance based on repair strategies. Ecoinvent 3.2 is a leading resource for life cycle inventory data, ensuring standardized, reliable assessments. It allows for comprehensive assessments covering impact categories such as global warming potential, eutrophication,

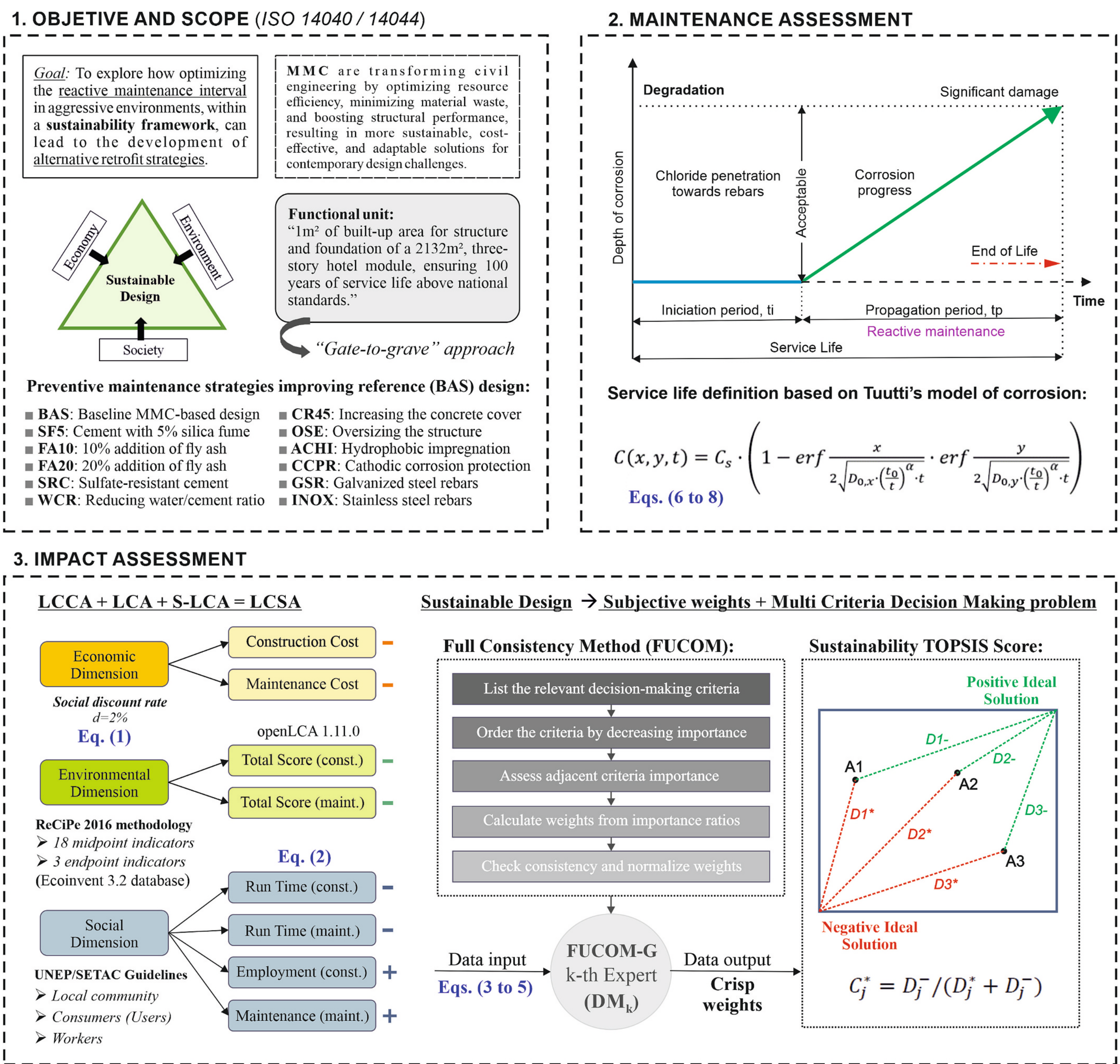

Fig. 3. Methodological framework.

Table 1
Material flows in each preventive design considered in the LCA during construction phase (initial impacts).

Inputs (per m^2 of structure)	BAS	SF5	FA10	FA20	SRC	WCR	CR45	ODSE	ACHI	CCRC	GALV	INOX
Pure/blended Portland cement (kg)	86.14	74.39	77.52	68.91	–	–	90.86	90.19	86.14	89.78	78.31	78.31
Marine-resistant cement (kg)	–	–	–		–	93.97	–	–	–	–	–	–
Sulphate-resisting cement (kg)	–	–	–	–	93.97	–	–	–	–	–	–	–
Water (liters)	51.68	50.90	51.68	51.68	46.98	51.68	54.51	54.11	51.68	54.08	46.98	46.98
Sand (kg)	213.00	213.00	213.00	213.00	207.99	207.99	224.66	223.02	213.00	213.00	213.00	213.00
Gravel (kg)	439.31	439.31	439.31	439.31	428.97	428.97	463.36	459.98	439.31	439.31	439.31	439.31
Silica fume (kg)	–	3.92	–	–	–	–	–	–	–	–	–	–
Fly ash (kg)	–	–	8.61	17.23	–	–	–	–	–	–	–	–
Silica aggregate (kg)	–	–	–	–	–	–	–	–	–	30.74	–	–
Titanium grid (kg)	–	–	–	–	–	–	–	–	–	0.57	–	–
Impregnation with silane (liters)	–	–	–	–	–	–	–	–	0.99	–	–	–
High-Density Polyethylene (m^3)						2.1579E-05[a]						
Reinforcement bars (kg)	27.51	27.51	27.51	27.51	27.51	27.51	27.51	34.40	27.51	27.51	–	–
Galvanized steel (kg)	–	–	–	–	–	–	–	–	–	–	33.55	–
Stainless steel (kg)	–	–	–	–	–	–	–	–	–	–	–	32.37
Transport, freight and lorry (t•km)	16.04	19.98	24.66	33.28	16.05	16.05	16.55	17.18	16.05	16.73	17.89	16.14

[a] The "cut-off criterion" applies to this material, as it is common to all alternatives.

Table 2
Material flows of each design according to the reactive maintenance strategy considered in the LCA.

Inputs (per m^2 of structure)	Damage level	BAS, SF5, FA10 FA20, SRC, WCR [b]	CR45 [c]	ODSE [d]	ACHI [b]	CCRC [d]	GALV [a]	INOX [a]
Thixotropic mortar 45 N/mm^2 (kg)	1	15.23	23.20	20.47	15.23	20.47	12.69	12.69
Water (liters)	1	1.46	2.37	2.06	1.46	2.06	1.17	1.17
Impregnation with silane (liters)	1	–	–	–	0.29	–	–	–
Transport, freight, lorry (t•km)	1	0.30	0.46	0.41	0.30	0.41	0.25	0.25
Thixotropic mortar 45 N/mm^2 (kg)	2	20.31	27.92	25.39	20.31	25.39	17.77	17.77
Water (liters)	2	2.04	3.50	2.63	2.04	2.63	1.75	1.75
Impregnation with silane (liters)	2	–	–	–	0.29	–	–	–
Aluminum silicate particle abrasive (kg)	2				1.13[e]			
Transport, freight, lorry (t•km)	2	0.40	0.55	0.50	0.40	0.50	0.35	0.35
Thixotropic mortar 45 N/mm^2 (kg)	3	25.39	33.00	30.46	25.39	30.46	22.85	22.85
Water (liters)	3	2.63	3.79	3.79	2.63	3.79	2.33	2.33
Impregnation with silane (liters)	3	–	–	–	0.29	–	–	–
Steel rebar UNE-EN 10080 B 500S (kg)	3	0.76	1.06	0.91	0.76	0.91	0.85	–
Zinc (10 % of the weight of rebar) (kg)	3	–	–	–	–	–	0.09	–
Transport, freight, lorry (t•km)	3	0.52	0.68	0.62	0.52	0.62	0.51	0.45

[a] Renovation of the concrete cover at 25, 35 and 45 mm for damage levels 1, 2 and 3, respectively (GALV, INOX).
[b] Restoration of the concrete cover at 30, 40 and 55 mm for damage levels 1, 2 and 3, respectively (BAS, SF5, FA10/20, SRC, WCR, ACHI).
[c] Restitution of the concrete cover at 40, 50 and 60 mm for damage levels 1, 2 and 3, respectively (CC45).
[d] Replacement of the concrete cover at 45, 55 and 65 mm for damage levels 1, 2 and 3, respectively (ODSE, CCRC).
[e] The "cut-off criterion" applies to this material, as it is common to all alternatives.

human toxicity, ozone depletion, and resource depletion. Table 3 maps the concepts to their equivalent flows in Ecoinvent.

In line with ISO 14044, a 1 % cut-off criterion was applied to exclude inventory flows with negligible influence on comparative sustainability outcomes. The following elements were omitted: (i) HDPE void formers and aluminum silicate abrasive, as they are common to all alternatives; (ii) local transport of conventional materials, such as concrete and steel, assumed to be sourced within a 50 km radius from standard suppliers and therefore non-differentiating; (iii) fuel and energy use associated with construction and maintenance equipment and machinery, excluded due to its invariance across all scenarios despite its potential absolute magnitude; and (iv) trichloroethylene solvent for rebar cleaning, whose impact was quantitatively below the 1 % threshold. Conversely, long-distance transport of special additives (e.g., silica fume and fly ash) was fully included due to their significant environmental contribution and variability across design options.

Key social factors were collected to define the social indicators in this evaluation model. The CYPE Ingenieros (2025) database provides crucial labor and machinery performance data, translating into execution time and labor hours. By analyzing task performance (work completed per hour or day), total project duration and labor demand can be estimated, including workforce requirements and job creation. This supports effective resource planning in construction. Table 4 presents activity values, with labor and machinery yields converted into equivalent performances using Eq. 2.

3. Maintenance prediction

3.1. Estimation of the service life of concrete elements

A damage model must be selected to predict and evaluate each design's maintenance requirements. Since the hotel is near the shore, chloride corrosion of the reinforcement is assumed to be the primary damage process. Predicting service life related to reinforcement corrosion is a growing discipline supported by mathematical models initially developed decades ago (Tuutti, 1982; Bakker, 1994; Fib, 2012). However, these models have not been extensively validated for concrete older than 30 years, and differences in historic cement and concrete composition limit their long-term accuracy. To assess durability, the Tuutti corrosion model is used (Tuutti, 1982) due to its wide acceptance,

Table 3
Ecoinvent datasets for modeling construction material data.

Inventory data concept	Equivalence with Ecoinvent dataset
Pure/blended Portland cement (kg)	Cement, Portland (kg) - Europe without Switzerland
Gravel (kg)	Gravel, crushed (kg) - GLO
Sand (kg)	Sand (kg) - GLO
Water (liters)	Tap water (kg) - Europe without Switzerland
Silica fume (kg)	Silica fume, densified (ecoinv) (kg) - GLO
Cement with 10 % fly ash addition	Cement, pozzolana and fly ash 5–15 %, US only (kg) - RoW
Cement with 20 % fly ash addition	Cement, pozzolana and fly ash 11–35 %, non-US (kg) - RoW
Sulphate-resisting cement (kg)	Cement, blast furnace slag 36–65 %, non-US (kg) - Europe without Switzerland
Marine-resistant cement (kg)	Cement, blast furnace slag 5–25 %, US only (kg) - RoW
Reinforcement bars B—500S (kg)	Reinforcing steel (kg) - RER
Impregnation silane (liters); $\gamma = 1{,}34$ Kg/m^3	Acrylic binder, without water, in 34 % solution state (kg) - RoW
Silica aggregate (kg)	Silica sand (kg) - RoW
Titanium grid (kg)	Titanium zinc plate, without pre-weathering (kg) - RoW
Galvanized steel (kg)	Zinc[a] (kg) - RoW + zinc oxide [a] (kg) - RoW
Stainless steel (kg)	Steel, chromium steel 18/8 (kg) - RER

[a] For every 100 kg of reinforcing steel, approx. 5–10 kg of the galvanizing mixture, consisting of 90 % zinc powder and 10 % zinc oxide, is added.

relative simplicity, and applicability to chloride-induced corrosion processes in reinforced concrete structures similar to the case study. Chloride-induced corrosion and damage to reinforcing bars follow specific stages during a concrete structure's lifespan (Hájková et al., 2018). Chloride penetration into the concrete occurs through capillary absorption in the surface layers and diffusion in deeper zones, leading to uneven corrosion that can sever steel bars and compromise structural integrity. According to Tuutti, the service life of a concrete element exposed to airborne chlorides has two stages (Fig. 4): the initiation period (t_i), where chlorides enter the concrete without affecting the reinforcement, and the propagation period (t_p), where chloride concentration is high enough to start corrosion of the steel.

While the Tuutti model provides a practical deterministic framework, other models like those developed within the DURACRETE project (Engelund et al., 2000) incorporate probabilistic and performance-based approaches. DURACRETE integrates variability in material properties and environmental exposure and incorporates limit states for corrosion initiation and propagation based on probabilistic durability concepts. Similarly, the CONTECVET manual (Fagerlund, 2001) proposes validated methodologies to assess residual life using both deterministic and probabilistic analyses, including stochastic modeling of chloride ingress and corrosion damage.

These more advanced models offer a physics-based and probabilistic description of corrosion damage states, addressing some of the limitations inherent in purely time-based deterministic models such as Tuutti's. However, given this study's data availability and objectives, the Tuutti model combined with a probabilistic framework following the Fib Model Code 2010 (Fib, 2012) is deemed appropriate to balance complexity and practical applicability. This approach quantifies material properties and environmental exposure uncertainties while maintaining manageable computational demands.

Diffusion-based models assume Fick's second law under non-stationary conditions, where chloride concentration $C(x,t)$ at any time (t) and depth (x) in the concrete cover is influenced by parameters like

Table 4
Equivalent yields (hours) during the construction (stage 0) and maintenance (stages 1, 2, 3) phases considered in S-LCA.

Construction unit	Phase	BAS, SF5, FA10 FA20, SRC, WCR	CR45	ODSE	ACHI	CCRC	GALV	INOX
Voided mat foundation (60 cm) (m^3)	0	220	267[a]	225 [b]	220	220	277[c]	273[d]
Biaxial voided slab (25 cm) + colums (m^2)	0	1088	1306[a]	1095[b]	1088	1088	1382 [c]	1370 [d]
Biaxial voided slab (30 cm) + colums (m^2)	0	533	664 [a]	537[b]	533	533	675 [c]	669 [d]
Hydrophobic impregnation (m^2)	0	–	–	–	304	–	–	–
Cathodic protection (m^2)	0	–	–	–	–	887	–	–
Surface preparation / concrete front (m^2)	1	476	604	599	476	476	476	476
Structural repair of concrete (m^2)	1	336	553	549	336	336	313	313
Hydrophobic impregnation (m^2)	1	–	–	–	304	–	–	–
Cathodic protection (m^2)	1	–	–	–	–	887	–	–
Repair of 25 cm slab fronts (m)	2	123	127	127	123	123	123	123
Repair of 30 cm slab fronts (m)	2	64	66	66	64	64	64	64
Concrete surface preparation (m^2)	2	512	512	512	512	512	512	512
Surface preparation of rebars (m^2)	2	113	113	113	113	113	113	113
Structural repair of concrete (m^2)	2	222	315	315	222	222	209	209
Hydrophobic impregnation (m^2)	2	–	–	–	304	–	–	–
Cathodic protection (m^2)	2	–	–	–	–	887	–	–
Repair of 25 cm slab fronts (m)	3	143	147	147	143	143	143	143
Repair of 30 cm slab fronts (m)	3	74	76	76	74	74	74	74
Concrete surface preparation (m^2)	3	512	512	512	512	512	512	512
Addition or replacement of rebars (m^2)	3	113	113	113	113	113	113	113
Structural repair of concrete (m^2)	3	469	603	603	469	469	419	419
Hydrophobic impregnation (m^2)	3	–	–	–	304	–	–	–
Cathodic protection (m^2)	3	–	–	–	–	887	–	–

[a] The total thickness of each slab is increased by a total of 3 cm due to the increase in covering.
[b] The total thickness of the mat foundations is oversized by 5 cm and that of each slab by 2 cm.
[c] 100 % more anchorage length and overlap for reinforcing steel (7850 kg/m^3) with a 6 % increase in weight due to the galvanizing bath.
[d] 100 % more anchorage length and overlap for stainless steel (specific weight of 8030 kg/m^3).

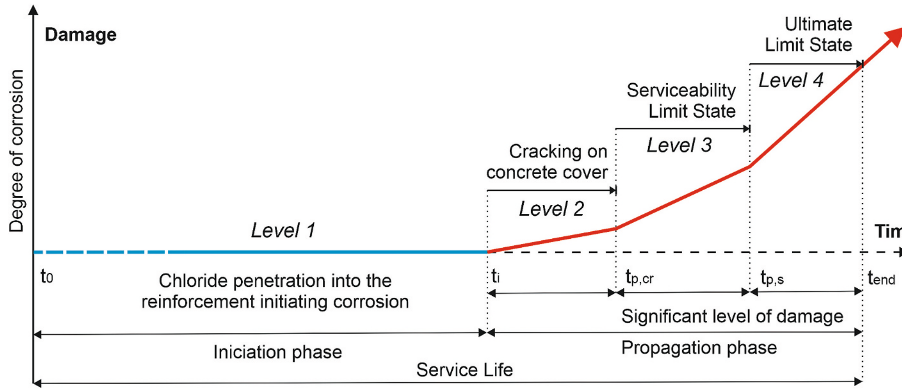

Fig. 4. Tuutti's theoretical model for corrosion progression.

surface chloride concentration, diffusion coefficient, and aging factors (Eq. 6) particularized for one-dimensional attack, i.e., without considering the so-called corner effects. While this simplification aligns with durability design standards such as the fib Model Code (2010), it may lead to underestimations in geometrically exposed zones. In particular, corner and edge effects may reduce corrosion initiation time by approximately 15–30 %, as Bastidas-Arteaga et al. (2013) reported. Nonetheless, 1D models remain widely accepted due to their conservative predictions and ease of application in large-scale assessments. However, these diffusion-based models are deterministic, relying on fixed parameters, and do not inherently incorporate material properties or environmental exposure uncertainties.

$$C(x,t) = C_s\left[1 - erf\frac{x}{2\sqrt{D_{0,x}\bullet\left(\frac{t}{t_0}\right)^{\alpha}\bullet t}}\right] \tag{6}$$

In this equation, C_s is defined as the surface chloride concentration (in % in weight of cement), $D_{0,x}$ is the effective chloride diffusion coefficient in concrete (m^2/s), t_0 is the reference time (0,0767 years), α is an aging coefficient (usually 0,5), and $erf(\cdot)$ is the error function. When the critical chloride limit (C_{cr}) is reached at the rebar cover, the initiation period ends, and the propagation period starts. This threshold is affected by the reinforcing steel's properties and is different between the alternatives under analysis.

The Fib Model Code 2010 (Fib, 2012) integrates probabilistic durability limit states to quantify risks, improve design robustness, and enhance durability predictions. This framework, which incorporates variability in environmental conditions, material heterogeneity, and corrosion kinetics, provides a more realistic and practical risk management approach for structures exposed to aggressive environments beyond the limitations of deterministic time-based models.

Considering the limitations inherent in purely time-based deterministic corrosion models, this study integrates Multi-Criteria Decision-Making (MCDM) methods, such as FUCOM-TOPSIS, to address uncertainties related to material properties, environmental exposure, and maintenance decisions. This approach combines physics-based corrosion modeling with probabilistic and multi-criteria decision-making methods, enhancing decision-making under uncertainty.

Given the uncertainties in corrosion initiation and propagation, probabilistic approaches provide a more realistic estimate of service life and failure probabilities, as the chloride-induced corrosion progressively diminishes the stiffness and cross-sectional area of the reinforcing steel. This probabilistic framework complements the deterministic diffusion models by quantifying risks associated with corrosion-induced failures. The duration from the initiation of corrosion to the cracking of the concrete cover ($t_{p,cr}$) can be predicted using the expression (Ministry of Transport, Mobility and Urban Agenda, 2021) shown in Eq. 7:

$$t_{p,cr} = \frac{80\bullet d}{\varnothing\bullet v_{corr}} \tag{7}$$

where Ø refers to the diameter of the rebar (in mm), d indicates the concrete cover (in mm), and v_{corr} denotes the corrosion velocity (in μm/year). Table 1 shows the durability parameters considered for each alternative, as well as the resulting initiation and propagation periods.

The propagation period (t_p) is defined as the time span from the onset of damage to the point where the inadmissible threshold marking the ultimate limit state is reached. The time elapsed from the initiation of corrosion to the reduction of the reinforcement cross-section ($t_{p,s}$) by a thickness $\Delta\Phi$ can be calculated using the equation below:

$$t_{p,s} = \frac{\Delta\Phi_{lim}}{v_{corr}} \tag{8}$$

Let $\Delta\Phi_{lim}$ represent the diameter change caused by reinforcement corrosion, deemed unacceptable, and measured in micrometers (μm). In this case, a cross-sectional loss of ≥15 % will be considered the threshold for replacement.

Table 5 summarizes the parameters and maintenance schedules necessary to evaluate the metrics and ensure the structure's durability over a 100-year lifespan for each alternative design. Despite these modeling efforts, significant uncertainty remains in long-term durability predictions, particularly for structures exposed to aggressive environments over several decades. This underscores the necessity of optimization frameworks that integrate uncertainty and sustainability criteria, as discussed in the following sections.

The key durability parameters and corresponding initiation (t_i) and propagation (t_p) times, calculated using Eqs. 7 and 8 within the chloride ingress diffusion model (Eq. 6), are compiled in Table 5. All parameter values are grounded in established normative references and literature to ensure non-arbitrariness and reproducibility.

- **Minimum cement contents (C_{min})** are determined according to exposure classes defined in the Structural Code (Ministry of Transport, Mobility and Urban Agenda, 2021), with adjustments for supplementary cementitious materials (SCMs) per Article 30 of EHE-08 (Ministry of Public Works, 2008). SCM contents comply with maximum limits: silica fume at 10 % and fly ash at 20 % by cement weight.
- **Critical chloride thresholds (C_{cr})** derive from Table A12.3.2.1.b of the Structural Code, which explicitly defines thresholds by protection type. Increased chloride limits are incorporated for galvanized, stainless steel, and other protection systems based on accepted standards and technical guidelines.
- **Surface chloride contents (C_s)** are sourced from Table A12.3.2.a of the Structural Code and converted to % concrete weight using the

Table 5
Durability model until the corrosion process is considered significant ($t_{ls} = t_i + t_p$) for each design alternative.

Parameters	BAS	SF5	FA10	FA20	SRC	WCR	CR45	ODSE	ACHI	CCPR	GALV	INOX
Model for the initiation period (t_i) in concrete elements.												
C_{min} (kg/m^3)	275	237.5[a]	247.5[b]	220[c]	300	300	275	275	275	275	250	250
C_{cr} (%)	0.6	0.6	0.6	0.6	0.6	0.6	0.6	0.6	0.6	0.9[e]	1.2[f]	1.4[h]
erf	0.752	0.817	0.800	0.849	0.713	0.713	0.753	0.752	0.753	0.557	0.453	0.362
C_s (%)	2.09	2.42	2.32	2.61	1.92	1.92	2.09	2.09	2.09	2.09	2.30	2.30
x (mm)	30	30	30	30	30	30	45	40	60[d]	40	25	25
D_0 (x10E-12 m^2/s)	14.9	4.8	9	6.9	6.9	10.9	14.9	14.9	25	25	14.9	14.9
t_0 (28 days in years)	0.077	0.077	0.077	0.077	0.077	0.077	0.077	0.077	0.077	0.077	0.077	0.077
α	0.5	0.5	0.5	0.5	0.5	0.5	0.5	0.5	0.5	0.5	0.5	0.5
t_i (years)	**9.3**	**64.5**	**20.0**	**26.8**	**53.8**	**21.6**	**47.0**	**29.4**	**52.8**	**34.7**	**34.2**	**83.8**
Models for the propagation period (t_p) in concrete elements up to the inadmissible loss of reinforcement diameter.												
d (mm)	30	30	30	30	30	30	45	40	60	40	25	25
Φ (mm)	12	12	12	12	12	12	12	16	12	12	12	12
v_{corr} (μm/year)	20	20	20	20	20	20	20	20	20	20	2[g]	1[i]
t_p (years)	**10**	**10**	**10**	**10**	**10**	**10**	**15**	**10**	**20**	**13.3**	**83.3**	**166.7**
t_{ls} (years)	**19.3**	**74.5**	**30.0**	**36.8**	**63.8**	**31.6**	**62.0**	**39.4**	**72.8**	**48.0**	**117.53**	**250.5**

[a] 12.5 kg/m^3 representing 5 % of silica fume in relation with 250 kg/m^2 of the C_{min}.
[b] 27.5 kg/m^3 representing to 10 % of fly ash in relation with 275 kg/m^2 of the C_{min}.
[c] 55 kg/m^3 representing to 20 % of fly ash in relation with 275 kg/m^2 of the C_{min}.
[d] Effective coating increase by multiplying by $\lambda = 1$ and adding it to the existing coating for a chloride rate of about 1.7 mm/half-day.
[e] 50 % increase in corrosion threshold due to corrosion inhibitor protection.
[f] Chloride ion limit contents in the case of reinforcements with additional hot-dip galvanized protection.
[g] The corrosion rate is 20 times lower if the reinforcing steel is galvanized (Moreno et al., 2005).
[h] Chloride ion limit contents in the case of stainless steel reinforcement.
[i] It is considered that there is no corrosion in the reinforcement, but we quantify the minimum of 1 μm/year for comparison.

standard unit weight of concrete (approximately 24 kN/m^3), ensuring consistency with normative procedures.

- **Concrete cover (x)** values follow Tables 43.4.1 and 44.2.1.1.b of the Structural Code. Special treatment adjustments include effective cover increases for ACHI as per Table A9.7 of EHE-08, and for CCPR, a bilayer coating of 40 mm thickness is incorporated to account for the cathodic protection system.
- **Diffusivity (D_0), aging coefficient (α), and corrosion rates (vc_{orr})** are assigned based on Tables A12.4.1 and A12.3.2.c of the Structural Code and supported by relevant literature (e.g., Moreno et al., 2005). Conservative corrosion rates, such as 1 μm/year for stainless steel, are used to maintain a consistent and fair comparison across alternatives.

A conceptual summary of the twelve building alternatives is provided in Table 6 below. This table synthesizes each solution's type, main intervention, underlying durability mechanism, and estimated service life (t_{ls}). Additionally, the table classifies the approach to maintenance (preventive, reactive, or hybrid), thereby clarifying each alternative's positioning within the life-cycle framework before the optimization analysis developed.

3.2. Optimal maintenance interval problem

Different forms of maintenance are defined depending on the degree of reinforcement damage at any given time to determine the optimal maintenance interval for each design. Table 7 outlines these actions and their corresponding damage conditions. If the evaluation time reaches the propagation period, the damage is unacceptable, and maintenance intervals exceeding t_p are disregarded. For a given evaluation time *(t)*, the maintenance-related economic, environmental, and social impacts (criteria C2, C4, C6, and C8) are calculated based on the necessary maintenance action. TOPSIS-FUCOM is then applied to rank each feasible maintenance interval by sustainability scoring, ensuring the selection of the most sustainable option by minimizing negative impacts.

The optimization process accounts for cumulative impacts over the

Table 6
Conceptual characterization of the twelve building alternatives.

Code	Design alternatives	Strategy	Key action or material	Durability mechanism	t_{ls} (years)
BAS[c]	Baseline design	Conventional	Standard RC	No enhancement; reference case	19.3
SF5[b]	5 % Silica fume	Mix design	Pozzolanic additive	Reduces permeability and improves microstructure	74.5
FA10[b]	10 % Fly ash	Mix design	Partial cement substitution	Enhances long-term strength and reduces CO_2	30.0
FA20[b]	20 % Fly ash	Mix design	Higher cement substitution	Further reduces clinker content	36.8
SRC[b]	Sulfate-resistant cement	Binder selection	Alternative cement binder	Improves chloride and sulfate resistance	63.8
WCR[b]	Water/cement ratio = 0.50	Mix design	Reduced water content	Lowers porosity and chloride diffusion	31.6
CR45[b]	Cover thickness 45 mm	Geometry	Increased concrete cover	Extends chloride penetration path	62.0
ODSE[b]	Oversize concrete & steel	Structural strength	+25 % material sections	Increases robustness and residual capacity	39.4
ACHI[b]	Hydrophobic impregnation	Surface treatment	Corrosion inhibiting layer	Blocks ingress and slows initiation of corrosion	72.8
CCPR[b]	Cathodic protection	Surface treatment	Electrochemical protection	Stops corrosion via electric current	48.0
GALV[a]	Galvanized steel rebars	Material change	Zinc-coated rebar	Sacrificial layer delays corrosion initiation	>100
INOX[a]	Stainless steel rebars	Material change	Corrosion-resistant alloy	Prevents corrosion initiation	> > 100

[a] Preventive (before damage occurs).
[b] Hybrid (preventive design plus later maintenance).
[c] Reactive (after detecting damage).

Table 7
Maintenance actions and damage conditions for optimal interval identification.

Maintenance	Intervention on the exterior perimeter and lower terrace slab areas	Damage status
Action 1	No maintenance required	$t < 50\ \%\ t_i$
Action 2	Hand-based surface preparation for structural concrete Structural repair of concrete with cement-based, polymer-modified mortar	$50\ \%\ t_i < t < t_i$
Action 3	Hand-based surface preparation for structural concrete Repair of the edge of RC slab, using mortar Surface preparation, restoration and protection of rebars in RC elements Structural repair of concrete surface, using polymer-modified cement-based mortar	$t_i < t < t_i + 50\ \%t_p$
Action 4	Hand-based surface preparation for structural concrete Repair of the edge of RC slab, using mortar Surface preparation, replacement and/or addition of rebars in RC elements Structural repair of concrete surface, using polymer-modified cement-based mortar	$t_i + 50\ \%t_p < t < t_p$

entire service life. That means that when evaluating a given maintenance interval t_k, impacts for categories C2, C4, C6, and C8 are assessed considering $n = t_l/t_k$ maintenance actions, where t_l is the evaluation period (namely 100 years). This approach ensures accurate cost estimation, applying discounting based on the timing of maintenance interventions.

4. Results and discussion

4.1. Economic performance results

Fig. 5 presents the Life Cycle Cost Assessment (LCCA) of the twelve design alternatives, considering unit construction costs per square meter and maintenance expenditures over a 100-year service period. This analysis balances initial investment with long-term upkeep, optimizing maintenance intervals to minimize life cycle impacts.

Sulforesistant cement (SRC) is the most cost-effective option, cutting costs by 65 % compared to the reference (BAS) and requiring repairs only every 53 years. Coating enhancement (CR45) and hydrophobic treatment (ACHI) follow closely with similar costs, while SF5 concrete ranks next. The top three options balance low maintenance and construction costs. SF5 has high upfront costs due to logistics but compensates with minimal maintenance, requiring just 1.5 repair cycles. Reactive solutions like CR45 and ACHI are cost-efficient, delaying repairs until severe deterioration (level 3). In contrast, SRC provides a more balanced preventive approach, intervening earlier (level 1) before reinforcement is needed.

The INOX option minimizes maintenance costs with its corrosion-resistant steel, lasting over 100 years without significant deterioration. However, its high construction cost—over twice the life-cycle cost of other alternatives—makes it less cost-effective. While the cheapest to build, BAS has the highest maintenance costs (37 % more than INOX), ranking as the second least preferred option. GALV offers similar durability to INOX with 30 % lower construction costs, providing a more balanced choice. Most alternatives, except special steels, have comparable construction costs (~71.50 €/m^2), with key differences emerging in maintenance, where repair cycles depend on durability (García-Segura et al., 2017). These findings underscore the importance of prioritizing long-term cost efficiency over initial investment.

This research adopts a deterministic framework for the LCCA, ensuring methodological rigor and clarity in the comparative evaluation of the twelve construction alternatives. Although state-of-the-art probabilistic approaches—such as those advanced by Otárola et al. (2024)—offer enhanced capabilities for capturing uncertainty and modeling complex multi-hazard interactions, their implementation necessitates extensive, high-fidelity data and computational complexity that currently exceeds the study's scope. The deterministic approach provides a robust, transparent, and replicable foundation aligned with the study's primary objectives. Future integration of probabilistic methodologies would further deepen the analysis, facilitating a more nuanced, risk-informed decision-making process and advancing the field toward comprehensive resilience assessment.

4.2. Environmental performance results

The environmental impacts of the 12 alternative designs, based on Life Cycle Assessment (LCA), are outlined in Fig. 6. The consequences on ecological integrity, human health, and resource depletion of the construction phase, which has the most significant impacts, are included. The maintenance phase, which has significantly lower impact scores, is presented as the total environmental footprint for graphical clarity.

Human health indicators account for around 40 % of the total environmental impact in all alternatives except INOX. For INOX, resource depletion during construction is the dominant factor, contributing 60 % of its impact—4.6 times higher than the average of other options. Ecosystem impact remains minimal across all designs. As a result, INOX has the highest overall environmental burden, which draws

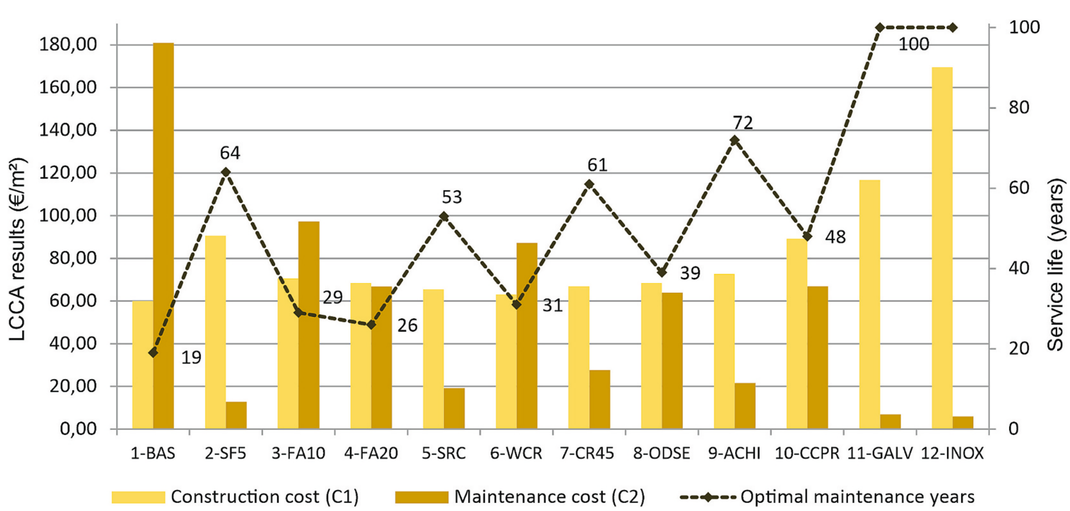

Fig. 5. Essential insights from the Life Cycle Cost Analysis.

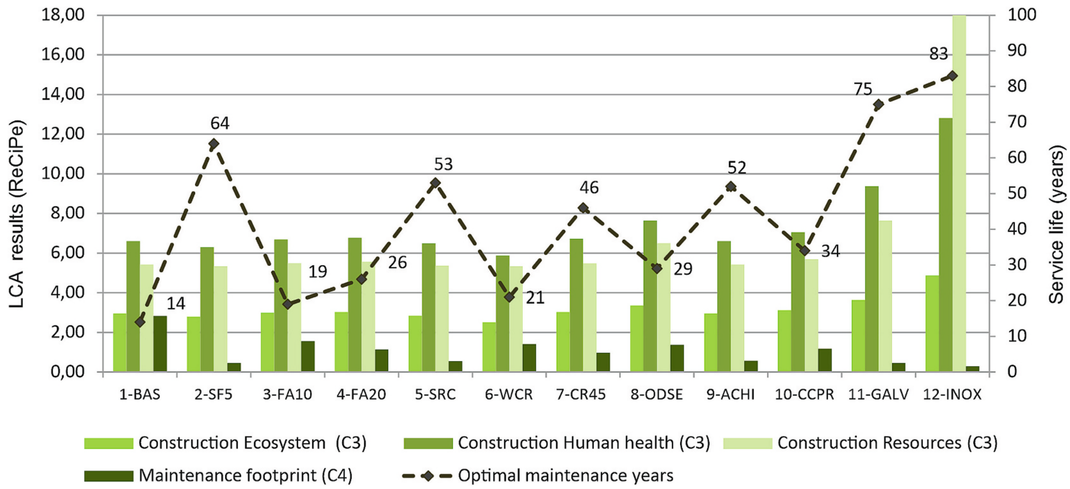

Fig. 6. Results derived from the Life Cycle Analysis.

attention to the ecological drawbacks of special corrosion-resistant alloy steelmaking, as highlighted by Mistry et al. (2016).

Higher durability does not always mean lower environmental impact. INOX and GALV represent the most extreme cases, while CR45 and ACHI, despite their long maintenance cycles of 46 and 52 years, still produce 7 % and 3 % more impact than WCR. With a shorter 29-year cycle, WCR is the most environmentally efficient maintenance option and the second-best overall, closely following SF5, the most eco-friendly design. Although WCR has 2.47 times more maintenance impact than ACHI due to lower durability, optimizing the water/cement ratio minimizes production impact by reducing the need for extra materials, additives, and protections. The best preventive designs—SF5, WCR, and SRC—reduce total environmental impact by 15–18 % compared to BAS, outperforming reactive maintenance strategies.

4.3. Social performance results

Fig. 7 illustrates the social impacts of construction and maintenance over time on three key stakeholders: workers, regional economic development, and local communities. Adverse effects on workers and public perception (C5 and C6) are assessed as construction times and maintenance cycles vary across alternatives. Meanwhile, employment generation and regional economic benefits (C7 and C8) are evaluated. The ideal solution minimizes C5 and C6 while maximizing C7 and C8. The social assessment framework by Sánchez-Garrido et al. (2021) is applied, capturing the structure's positive societal contributions throughout its life cycle.

Regarding negative impacts, most alternatives share similar construction times, except those with concrete mix improvements (BAS, SF5, FA10/20, SRC, and WCR). Differences mainly arise in maintenance and repair cycles. The baseline design (BAS) has the highest maintenance impact, requiring frequent repairs every 19 years, with 5.26 cycles before structural failure. Cathodic corrosion protection (CCPR) follows, despite a longer 48-year interval, due to its labor-intensive maintenance, involving mortar removal, titanium mesh replacement, and power cable adjustments, making it the second most time-consuming option.

Socially, the best-performing design is SF5, with a 64-year durability due to silica fume. It is followed by sulfate-resistant cement (SRC) at 53 years, while GALV and INOX steels lead with minimal maintenance needs and optimal 100- and 83-year intervals. These long-lasting solutions reduce worker risks, accessibility issues, user inconvenience, and negative public perception, achieving the highest social scores.

Options involving intricate production methods, like specialized steel fabrication, incremental coatings requiring additional reinforcement against shrinkage (CR45), or cathodic protection (CCPR),

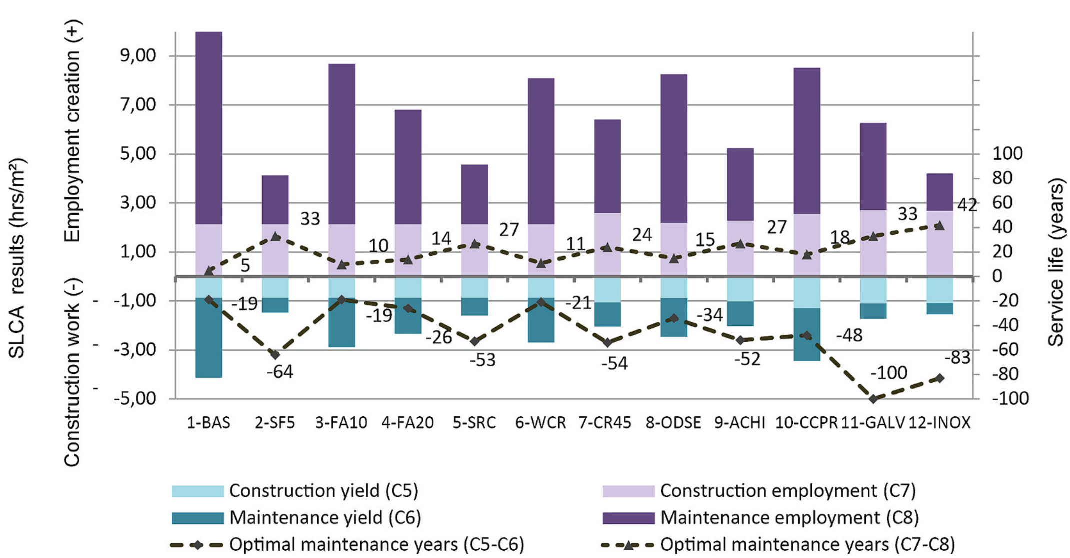

Fig. 7. Findings from the Social Life Cycle Analysis.

Table 8
FUCOM group crisp weight.

Sustainability dimension	Criterion	Weighting of the criteria obtained by each decision maker by importance and comparative priority.						FUCOM-G
		wDM_1	δDM_1	wDM_2	δDM_2	wDM_3	δDM_3	
Economy	(C1) Building cost (construction)	0.164	0.561	0.179	0.617	0.235	0.856	0.198
	(C2) Repair cost (maintenance)	0.263		0.077		0.181		0.172
Environment	(C3) Endpoint impact (construction)	0.088	0.561	0.269	0.617	0.094	0.856	0.145
	(C4) Endpoint impact (maintenance)	0.066		0.090		0.078		0.078
Society	(C5) Deadline (construction)	0.219	0.561	0.054	0.617	0.156	0.856	0.143
	(C6) Deadline (maintenance)	0.044		0.067		0.130		0.087
	(C7) Employment (construction)	0.105		0.158		0.067		0.105
	(C8) Employment (maintenance)	0.053		0.107		0.059		0.072

significantly impact workers and the regional economy during construction. The material used depends on maintenance frequency rather than construction methods. BAS has the highest positive social impact, with repairs every five years. Though it lacks preventive measures and performs poorly in construction, it generates twice the employment of the following best option, FA10 (10 % fly ash). High material demands over time drive job creation and economic activity, as noted by Navarro et al. (2018). Fig. 7 reflects this, showing shorter positive (+) social maintenance intervals than negative (−) ones, as optimal maintenance occurs early in the service life when the first coating replacement is required ($t \geq 50\ \%\ t_i$), leading to frequent cycles.

4.4. Sustainability-oriented approach

Each alternative underwent a rigorous assessment within a structured framework considering sustainability's three key environmental, economic, and social dimensions. The FUCOM technique was employed to prioritize impact categories based on expert insights. A fuzzy function, inspired by Sánchez-Garrido et al. (2024b) and derived from the neutrosophic function by Sodenkamp et al. (2018), was used to determine the influence of each expert's vote. This method considers professional experience, perceived competence, and assessment consistency. The resulting expert weightings, reflecting their voting influence, are shown in Table 8 for the eight evaluated criteria. The results indicate that social criteria are considered the most important, accounting for nearly 41 %, followed by economic (37 %) and environmental (22 %) criteria. The predominance of social criteria reflects the contextual relevance of stakeholder-oriented indicators in active-use buildings. In the case of a coastal hotel with continuous occupancy, experts prioritized time-sensitive and labor-related factors to reduce user disruption and ensure the technical and logistical viability of sustainable rehabilitation under operational constraints.

The TOPSIS method was applied to determine the optimal maintenance interval that maximizes sustainability scores based on the assigned criteria weights. Table 9 presents the decision matrix, mapping the 12 design options to their scores across eight impact categories. Fig. 8 visualizes the sustainability scores for each design under the optimal reactive maintenance interval, with minimized criteria (C1–C6) shown above the x-axis and maximized criteria (C7, C8) below.

The most sustainable option, with an index of 0.82, is sulfur-resistant cement (SRC). While SRC did not lead in individual environmental or social impact assessments, it offers a well-balanced, durable design with a 53-year maintenance interval. Hydrophobic impregnation (ACHI) and the 5 % silica fume mix (SF5) follow closely, both scoring 0.80 with intervals of 62 and 63 years. In contrast, the least sustainable option, the baseline design (BAS), lacks preventive measures and scores just 0.44—up to 86.4 % lower than SRC.

With a 100-year interval, the maintenance-free INOX option improves sustainability by only 27 % over the reference (BAS), proving that avoiding maintenance does not always enhance sustainability. Except for GALV, INOX significantly increases economic (doubling) and environmental (tripling) impacts during construction, making it the second least favorable choice. Maintenance intervals vary widely, with less durable options like BAS, FA10/20, WCR, and ODSE reaching end-of-life (EoL) between 19 and 39 years—below the 50-year regulatory minimum. In these cases, it is more effective to adopt a reactive maintenance approach that maximizes proximity to EoL with optimal repair cycles every 19, 18/20, 26 and 34 years.

Some designs balance preventive and reactive strategies effectively. CR45, for instance, extends EoL to 61 years by increasing concrete cover from 30 to 45 mm. With a single repair at year 57, it surpasses 100 years of service life, ranking fourth in sustainability. Though SF5 performs better overall, its sustainability is weakened by poor social performance, as silica fume must be transported over 1000 km from La Coruña, Spain.

Table 9
Ultimate decision-making step employing the TOPSIS technique.

C_k	1 BAS	2 SF5	3 FA10	4 FA20	5 SRC	6 WCR	7 CR45	8 ODSE	9 ACHI	10 CCPR	11 GALV	12 INOX	Opt.
C1	60.074	90.656	70.620	68.511	65.501	63.137	66.878	68.469	72.776	89.184	116.762	169.485	Min.
C2	180.921	16.503	105.070	66.843	24.410	102.621	32.008	74.094	28.065	85.016	12.866	5.882	Min.
C3	14.999	14.439	15.182	15.367	14.690	13.737	15.223	17.497	14.999	15.859	20.656	44.021	Min.
C4	3.886	0.574	1.563	1.142	0.683	1.523	1.724	1.456	0.639	1.207	0.462	0.346	Min.
C5	0.868	0.868	0.868	0.868	0.868	0.868	1.055	0.890	1.012	1.286	1.100	1.089	Min.
C6	3.256	0.708	2.014	1.472	0.842	1.879	1.089	1.571	1.019	2.211	0.706	0.529	Min.
C7	2.133	2.133	2.133	2.133	2.133	2.133	2.591	2.191	2.277	2.552	2.707	2.681	Max.
C8	5.973	1.509	3.449	2.521	1.796	4.006	1.991	3.338	1.911	3.560	1.371	1.028	Max.
D_j^*	0.129	0.038	0.072	0.050	0.033	0.068	0.040	0.053	0.034	0.065	0.052	0.102	–
D_j^-	0.101	0.146	0.110	0.126	0.148	0.117	0.138	0.120	0.143	0.109	0.138	0.129	–
Q_j^* [a]	**0.440**	**0.794**	**0.606**	**0.717**	**0.819**	**0.630**	**0.777**	**0.693**	**0.806**	**0.626**	**0.727**	**0.559**	–
Ranking	12th	3rd	10th	6th	*1st*	8th	4th	7th	2nd	9th	5th	11th	–

[a] Highest score better (farthest from the ideal negative solution).

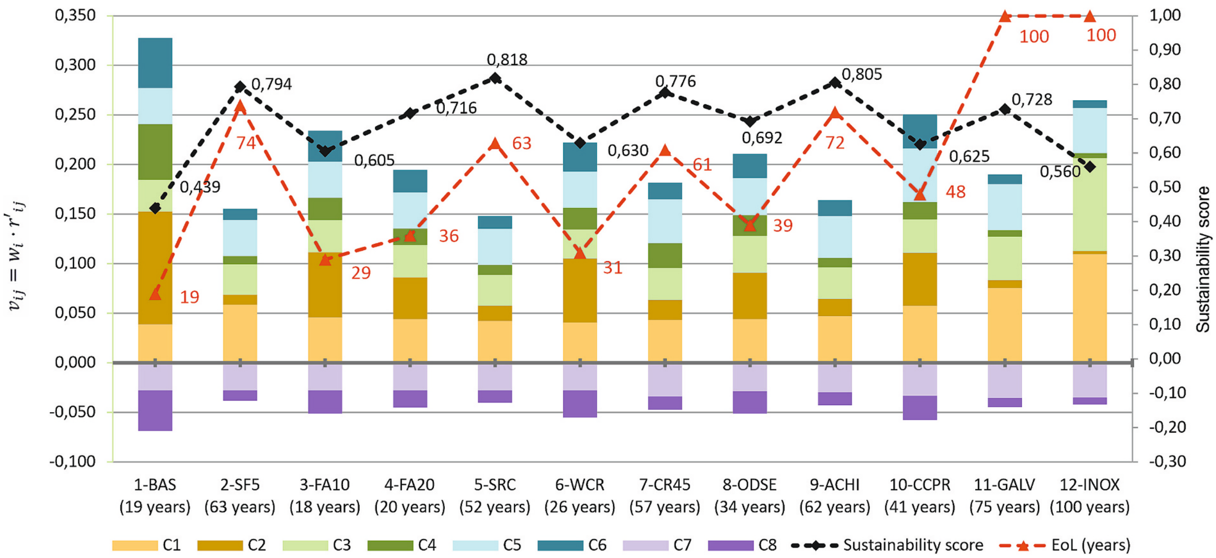

Fig. 8. Assessment results evaluating all three dimensions of sustainability.

The absence of a direct link between individual assessments (LCCA, LCA, and S-LCA) and a three-dimensional sustainability approach emphasizes the need for an integrated design strategy that considers all aspects simultaneously. The findings align with those of Navarro et al. (2019) and Nolan et al. (2021), highlighting the limitations of traditional sustainability assessments that focus only on economic and environmental factors. While these bi-dimensional approaches have typically guided decision-making, they overlook the critical role of social impact in achieving true sustainability. Given the issue's complexity, a comprehensive structural design evaluation must fully incorporate the social dimension beyond just economic-environmental trade-offs. This ensures that sustainability strategies foster long-term societal well-being alongside financial and ecological responsibility.

5. Conclusions

This paper conducts a holistic life cycle assessment under ISO 14040 to compare 12 MMC-based structural designs for the preventive maintenance of a coastal hotel building. The analysis evaluates economic, environmental, and social impacts over a 100-year service life, precisely defining the functional unit and product system. Sustainability was assessed using the TOPSIS technique across eight impact categories, with FUCOM experts determining the importance of the criterion. The process began by identifying optimal ranges for sustainable reactive maintenance based on annual deterioration and repair strategies. Finally, the 12 solutions were evaluated by comparing one-dimensional sustainability metrics with a comprehensive three-dimensional approach.

In aggressive environments, more excellent durability generally improves sustainability. However, this is not always true when durability relies on preventive strategies that modify the concrete mix. The most sustainable options use silica fume or sulfate-resistant cement, achieving high durability (74 and 63 years EoL) while reducing impacts by 30 % and 40 %, respectively. In contrast, adding fly ash or lowering the water/cement ratio increases durability by only 10 to 17 years over the reference design.

Notably, the most sustainable option (SRC) is not the one with the most extended service life (GALV or INOX) but the one that best balances sustainability (0.81 index), maintenance optimization (52-year intervals), and durability. When incorporating alternative durability strategies—such as non-conventional steels or protective measures like cathodic protection—low maintenance does not always mean higher sustainability, nor do high-maintenance solutions necessarily perform poorly. Maintenance-free options, like stainless steel, performed 30 % worse than reactive maintenance approaches involving periodic hydrophobic surface treatments or thicker reinforcement coatings.

The expert panel identified the social dimension as the most influential factor in sustainable structural design, with a weight of 41 %. Though often overlooked, this study demonstrates that integrating social aspects into life cycle assessments leads to more effective designs, especially in aggressive environments requiring frequent maintenance.

Results show that one-dimensional assessments can miss critical factors, resulting in suboptimal design choices. Considering the link between material selection and repair strategies—beyond initial costs or immediate environmental impact—is essential. While some construction options may have higher upfront costs, they can lower maintenance needs, extend service life, and reduce long-term costs and environmental impact. Additionally, these choices enhance structural reliability, minimize repair-related disruptions (crucial for hotel operations), and improve user safety and community well-being.

Future research will focus on two main areas: developing AI and machine learning models to improve concrete degradation predictions beyond current regulations and optimizing maintenance intervals. Building on these advancements, it will compare the sustainability and effectiveness of preventive versus reactive maintenance in chloride-exposed concrete structures. This work underscores the challenges of designing durable concrete structures for harsh environments, emphasizing the importance of balancing preventive strategies with reactive maintenance planning to achieve long-term sustainability.

Declaration of competing interest

The authors whose names are listed immediately below certify that they have NO affiliations with or involvement in any organization or entity with any financial interest (such as honoraria; educational grants; participation in speakers' bureaus; membership, employment, consultancies, stock ownership, or other equity interest; and expert testimony or patent-licensing arrangements), or non-financial interest (such as personal or professional relationships, affiliations, knowledge or beliefs) in the subject matter or materials discussed in this manuscript.

This statement is signed by all the authors to indicate agreement that the above information is true and correct.

Acknowledgments

Grant PID2023-150003OB-I00 funded by MICIU/AEI/10.13039/501100011033 and by "ERDF/EU".

The authors wish to express their appreciation to the companies that supplied pertinent data and information essential for this study, with special acknowledgment to UNIDOME Deutschland GmbH.

Appendix A. Appendix

Table A.1
Building alternatives characterization based on construction costs for Life Cycle Cost Assessment.

Alternative	Item description	Cost	Unit
All designs	Multiaxial concrete shapers "Unidome XS-D420 (470)" for level 0	7.13	€/m^2
	Multiaxial concrete shapers "Unidome" XS-120 (150)" for levels 1 and 2	6.85	€/m^2
	Multiaxial concrete shapers "Unidome XS-160 (190)" for level 3	8.56	€/m^2
1 – BAS	Mat foundation (level 0) 60 cm (25 Mpa) and steel (60 kg/m^3)	210.05	€/m^3
9 – ACHI	LRCS[a] (levels 1 and 2) 25 cm (25 Mpa) and steel (26 kg/m^2)	135.87	€/m^2
10 – CCPR	LSRCS[a] (level 3) 30 cm (25 Mpa) and steel (22 kg/m^2)	131.57	€/m^2
2 – SF5	Mat foundation (level 0) 60 cm +5 % SF[b] (25 Mpa) and steel (60 kg/m^3)	331.85	€/m^3
	LRCS[a] (levels 1 and 2) 25 cm +5 % SF[b] (25 Mpa) and steel (26 kg/m^2)	214.67	€/m^2
	LRCS[a] (level 3) 30 cm +5 % SF[a] (25 Mpa) and steel (22 kg/m^2)	207.88	€/m^2
3 – FA10	Mat foundation 60 cm (level 0) +10 % FA[c] (25 Mpa) and steel (60 kg/m^3)	256.20	€/m^3
	LRCS[a] (levels 1 and 2) 25 cm +10 % FA[c] (25 Mpa) and steel (26 kg/m^2)	165.76	€/m^2
	LRCS[a] (level 3) 30 cm +10 % FA[c] (25 Mpa) and steel (22 kg/m^2)	160.52	€/m^2
4 – FA20	Mat foundation (level 0) 60 cm +20 % FA[c] (25 Mpa) and steel (60 kg/m^3)	254.10	€/m^3
	LRCS[a] (levels 1 and 2) 25 cm +20 % FA[c] (25 Mpa) and steel (26 kg/m^2)	164.40	€/m^2
	LRCS[a] (level 3) 30 cm +20 % FA[c] (25 Mpa) and steel (22 kg/m^2)	159.20	€/m^2
5 – SRC	Mat foundation (level 0) 60 cm (30 Mpa – SR[d]) and steel (60 kg/m^3)	239.69	€/m^3
	LRCS[a] (levels 1 and 2) 25 cm (30 Mpa – SR[d]) and steel (26 kg/m^2)	142.75	€/m^2
	LRCS[a] (level 3) 30 cm (30 Mpa – SR[d]) and steel (22 kg/m^2)	139.45	€/m^2
6 – WCR	Mat foundation (level 0) 60 cm (30 Mpa – MR[e]) and steel (60 kg/m^3)	230.77	€/m^3
	LRCS[a] (levels 1 and 2) 25 cm (30 Mpa – MR[e]) and steel (26 kg/m^2)	136.62	€/m^2
	LRCS[a] (level 3) 30 cm (30 Mpa – MR[e]) and steel (22 kg/m^2)	132.43	€/m^2
7 – CR45	Mat foundation (level 0) 63 cm (25 Mpa) and steel (57 kg/m^3)	218.47	€/m^3
	LRCS[a] (levels 1 and 2) 28 cm (25 Mpa) and steel (26 kg/m^2)	151.52	€/m^2
	LRCS[a] (level 3) 33 cm (25 Mpa) and steel (22 kg/m^2)	146.94	€/m^2
8 – ODSE	Mat foundation (level 0) 65 cm (25 Mpa) and steel (69 kg/m^3)	233.15	€/m^3
	LRCS[a] (levels 1 and 2) 27 cm (25 Mpa) and steel (35.2 kg/m^2)	148.28	€/m^2
	LRCS[a] (level 3) 32 cm (25 Mpa) and steel (27.5 kg/m^2)	145.12	€/m^2
9 – ACHI	+ Anti-corrosion hydrophobic impregnation (terraces in levels 1,2 and 3)	+50.54	€/m^2
10 – CCRC	+ Cathodic corrosion protection of RC (idem above)	+115.83	€/m^2
11 – GALV	Mat foundation (level 0) 60 cm (25 Mpa) and galvanized steel (68 kg/m^3)	315.48	€/m^3
	LRCS[a] (levels 1 and 2) 25 cm (25 Mpa) and galvanized steel (29.5 kg/m^2)	181.58	€/m^2
	LRCS[a] (level 3) 30 cm (25 Mpa) and galvanized steel (25 kg/m^2)	170.25	€/m^2
12 – INOX	Mat foundation (level 0) 60 cm (25 Mpa) and stainless steel (65.5 kg/m^3)	604.80	€/m^3
	LRCS[a] (levels 1 and 2) 25 cm (25 Mpa) and stainless steel (28.5 kg/m^2)	391.31	€/m^2
	LRCS[a] (level 3) 30 cm (25 Mpa) and stainless steel (24 kg/m^2)	378.72	€/m^2

LRCS [a] = Lightweight RC slabs; SF [b] = Silica fume; FA[c] = Fly ash; SR[d] = Cement resistant to sulfates; MR[e] = Cement with marine-grade resistance.

Table A.2
Characterization of maintenance actions and costs by maintenance level (LM) in the Life Cycle Cost Assessment.

Altern.	LM	Item description	Cost	Unit
All	1	Manual surface cleaning and preparation of concrete structures (20 mm)	36.60	€/m^2
	2,3	Manual surface cleaning and preparation of concrete structures (40 mm)	45.75	€/m^2
	2,3	Surface preparation of reinforcement in RC elements	8.68	€/m^2
1 – BAS	1	Structural concrete repair, with cement-based, polymer-modified mortar (30 mm)	63.07	€/m^2
2 – SF5	2	Repair of RC slab front (25 cm thick), with mortar (30 + 10 mm)	66.50	€/m
3 – FA10	2	Repair of RC slab front (30 cm thick), with mortar (30 + 10 mm)	71.42	€/m
4 – FA20	2	Structural concrete repair, with cement-based, polymer-modified mortar (30 + 10 mm)	82.07	€/m^2
5 – SRC	3	Repair of RC slab front (25 cm thick), with concrete (30 + 20 mm)	76.13	€/m
6 – WCR	3	Repair of RC slab front (30 cm thick), with concrete (30 + 20 mm)	77.15	€/m
9 – ACHI	3	Structural concrete repair, with cement-based, polymer-modified mortar (30 + 20 mm)	98.64	€/m^2

(*continued on next page*)

Table A.2 (*continued*)

Altern.	LM	Item description	Cost	Unit
7 – CR45	1	Structural concrete repair, with cement-based, polymer-modified mortar (45 mm)	91.49	€/m^2
	2	Repair of RC slab front (28 cm thick), with mortar (45 + 10 mm)	78.00	€/m
	2	Repair of RC slab front (33 cm thick), with mortar (45 + 10 mm)	82.26	€/m
	2	Structural concrete repair, with cement-based, polymer-modified mortar (45 + 10 mm)	105.78	€/m^2
	3	Repair of RC slab front (28 cm thick), with concrete (45 + 20 mm)	80.36	€/m
	3	Repair of RC slab front (33 cm thick), with concrete (45 + 20 mm)	81.06	€/m
	3	Structural concrete repair, with cement-based, polymer-modified mortar (45 + 20 mm)	120.06	€/m^2
8 – ODSE	1	Structural concrete repair, with cement-based, polymer-modified mortar (40 mm)	84.35	€/m^2
	2	Repair of RC slab front (27 cm thick), with mortar (40 + 10 mm)	68.49	€/m
	2	Repair of RC slab front (32 cm thick), with mortar (40 + 10 mm)	78.90	€/m
	2	Structural concrete repair, with cement-based, polymer-modified mortar (40 + 10 mm)	98.64	€/m^2
	3	Repair of RC slab front (27 cm thick), with concrete (40 + 20 mm)	78.39	€/m
	3	Repair of RC slab front (32 cm thick), with concrete (40 + 20 mm)	79.52	€/m
	3	Structural concrete repair, with cement-based, polymer-modified mortar (40 + 20 mm)	112.92	€/m^2
9 – ACHI	1,2,3	+ Anti-corrosion hydrophobic impregnation (terraces in levels 1,2 and 3)	+50.54	€/m^2
10 – CCPR	1	Structural concrete repair, with cement-based, polymer-modified mortar (30 + 10 mm)	84.35	€/m^2
	2	Repair of RC slab front (25 cm thick), with mortar (30 + 10 + 10 mm)	68.49	€/m
	2	Repair of RC slab front (30 cm thick), with mortar (30 + 10 + 10 mm)	78.90	€/m
	2	Structural concrete repair, with cement-based, polymer-modified mortar (40 + 10 mm)	98.64	€/m^2
	3	Repair of RC slab front (25 cm thick), with concrete (30 + 20 + 10 mm)	78.39	€/m
	3	Repair of RC slab front (30 cm thick), with concrete (30 + 20 + 10 mm)	79.52	€/m
	3	Structural concrete repair, with cement-based, polymer-modified mortar (30 + 20 + 10 mm)	112.92	€/m^2
	1,2,3	+ Cathodic corrosion protection of RC	+115.83	€/m^2
11 – GALV 12 – INOX[a]	1	Structural concrete repair, with cement-based, polymer-modified mortar (25 mm)	55.09	€/m^2
	2	Repair of RC slab front (25 cm thick), with mortar (25 + 10 mm)	63.96	€/m
	2	Repair of RC slab front (30 cm thick), with mortar (25 + 10 mm)	68.37	€/m
	2	Structural concrete repair, with cement-based, polymer-modified mortar (25 + 10 mm)	75.60	€/m^2
	3	Repair of RC slab front (25 cm thick), with concrete (25 + 20 mm)	84.19	€/m
	3	Repair of RC slab front (30 cm thick), with concrete (25 + 20 mm)	85.38	€/m
	3	Structural concrete repair, with cement-based, polymer-modified mortar (25 + 20 mm)	91.49	€/m^2

INOX [a] = Stage 3 maintenance is not taken into account in the evaluation of this alternative, since the steel does not corrode.

Data availability

Data will be made available on request.

References

Ait-Ali, A., Odolinski, K., Pålsson, B., Torstensson, P., 2024. Evaluating the mix of maintenance activities on railway crossings with respect to life-cycle costs. Eur. J. Transp. Infrastruct. Res. 24 (1), 1–29. https://doi.org/10.59490/ejtir.2024.24.1.6885.

Alba-Rodríguez, M.D., Martínez-Rocamora, A., González-Vallejo, P., Ferreira-Sánchez, A., Marrero, M., 2017. Building rehabilitation versus demolition and new construction: economic and environmental assessment. Environ. Impact Assess. Rev. 66, 115–126. https://doi.org/10.1016/j.eiar.2017.06.002.

Alhassan, M., Al-Rousan, R., Shatnawi, A., 2022. Experimental evaluation of the shear strength of the unidome slab system. In: CESARE Conference Publications: 3rd Coordinating Engineering for Sustainability and Resilience (May 6th–9th, 2022, Irbid, Jordan) (ISSN 2788-6204).

Ascione, F., De Masi, R.F., Mastellone, M., Vanoli, G.P., 2022. Building rating systems: a novel review about capabilities, current limits and open issues. Sustain. Cities Soc. 76, 103498. https://doi.org/10.1016/j.scs.2021.103498.

Bakker, R.F.M., 1994. Prediction of service life reinforcement in concrete under different climatic conditions at given cover. In: Swamy, R.N. (Ed.), Corrosion and Protection of Steel in Concrete: Proceedings of the International Conference, Sheffield, U.K., 24–28 July 1994 (Vol. 1, Pp. 527–539). Sheffield Academic Press (ISBN 978-1853123285).

Bastidas-Arteaga, E., Schoefs, F., 2015. Sustainable maintenance and repair of RC coastal structures. Proc. Inst. Civil Eng. 168, 162–173. https://doi.org/10.1680/jmaen.14.00018.

Bastidas-Arteaga, E., Schoefs, F., Stewart, M.G., Wang, X., 2013. Influence of global warming on durability of corroding RC structures: a probabilistic approach. Eng. Struct. 51, 259–266. https://doi.org/10.1016/j.engstruct.2013.01.006.

Boardman, A.E., Greenberg, D.H., Vining, A.R., Weimer, D.L., 2018. Cost-Benefit Analysis: Concepts and Practice, 5th ed. Cambridge University Press (ISBN 978–1108401296).

Bru, D., González, A., Baeza, F.J., Ivorra, S., 2018. Seismic behavior of 1960's RC buildings exposed to marine environment. Eng. Fail. Anal. 90, 324–340. https://doi.org/10.1016/j.engfailanal.2018.02.011.

Choi, J., 2019. Strategy for reducing carbon dioxide emissions from maintenance and rehabilitation of highway pavement. J. Clean. Prod. 209, 88–100. https://doi.org/10.1016/j.jclepro.2018.10.226.

CYPE Ingenieros, 2025. Construction Price Generator. Spain. https://generadordeprecios.info/.

Del Serrone, G., Riccio, G., Moretti, L., 2025. Cradle-to-cradle life cycle assessment of railway prestressed concrete sleepers: a state-of-the-art review and strategies for reducing environmental impacts. Resour. Conserv. Recycl. 214, 108020. https://doi.org/10.1016/j.resconrec.2024.108020.

Di Summa, D., Parpanesi, M., Ferrara, L., De Belie, N., 2023. A holistic life cycle design approach to enhance the sustainability of concrete structures. Struct. Concr. 24 (6), 7684–7704. https://doi.org/10.1002/suco.202300645.

Ding, Z., Huang, X., Wang, X., Zuo, J., 2025. Assessment of promotional strategies for construction and demolition waste recycled products based on hybrid simulation system. Environ. Impact Assess. Rev. 112, 107814. https://doi.org/10.1016/j.eiar.2025.107814.

Engelund, S., Mohr, L., Edvardsen, C., DuraCrete Consortium, 2000. General Guidelines for Durability Design and Redesign: DuraCrete, Probabilistic Performance-Based Durability Design of Concrete Structures (Final Technical Report, Document BE95–1347/R15). CUR. https://es.scribd.com/document/806509883/Duracrete-2000.

Fagerlund, G. (Ed.), 2001. CONTECVET: A Validated User's Manual for Assessing the Residual Service Life of Concrete Structures (Report TVBM-7161). Division of Building Materials, Lund University. Recuperado de. https://www.ietcc.csic.es/wp-content/uploads/1989/02/manual_contecvet_ingles.pdf.

Fédération internationale du béton (Fib), 2012. fib Model Code for Concrete Structures 2010. Fédération internationale du béton (fib). https://www.fib-international.org/publications/fib-bulletins/model-code-2010-final-draft%2C-volume-1-detail.html.

Frangopol, D.M., Dong, Y., Sabatino, S., 2017. Bridge life-cycle performance and cost: analysis, prediction, optimisation and decision-making. Struct. Infrastruct. Eng. 13 (10), 1239–1257. https://doi.org/10.1080/15732479.2016.1267772.

García-Segura, T., Yepes, V., Frangopol, D., Yang, D.Y., 2017. Lifetime reliability based optimization of post-tensioned box-girder bridges. Eng. Struct. 145, 381–391. https://doi.org/10.1016/j.engstruct.2017.05.013.

Hadizadeh-Bazaz, M., Navarro, I.J., Yepes, V., 2023. Life cycle assessment of a coastal concrete bridge aided by non-destructive damage detection methods. J Mar Sci Eng 11 (9), 1656. https://doi.org/10.3390/jmse11091656.

Hájková, K., Šmilauer, V., Jendele, L., Červenka, J., 2018. Prediction of reinforcement corrosion due to chloride ingress and its effects on serviceability. Eng. Struct. 174, 768–777. https://doi.org/10.1016/j.engstruct.2018.08.006.

Han, X., Frangopol, D.M., 2022. Risk-informed bridge optimal maintenance strategy considering target service life and user cost at project and network levels. ASCE-ASME J. Risk Uncertain. Eng. Syst. A 8 (4), 04022050. https://doi.org/10.1061/AJRUA6.00012.

Haqbin, M., 2022. Comparing best-worst method and full consistency method in a fuzzy environment. Decis. Sci. Lett. 11, 181–192. https://doi.org/10.5267/dsl.2021.11.002.

Hu, J.Y., Zhang, S.S., Chen, E., Li, W.G., 2022. A review on corrosion detection and protection of existing reinforced concrete (RC) structures. Construct. Build Mater. 325, 126718. https://doi.org/10.1016/j.conbuildmat.2022.126718.
Huijbregts, M.A.J., Steinmann, Z.J.N., Elshout, P.M.F., Stam, G., Verones, F., Vieira, M., Zijp, M., Hollander, A., Van Zelm, R., 2017. ReCiPe2016: a harmonised life cycle impact assessment method at midpoint and endpoint level. Int. J. Life Cycle Assess. 22, 138–147. https://doi.org/10.1007/s11367-016-1246-y.
Hwang, C.L., Yoon, K., 1981. Multiple Attribute Decision Making: Methods and Applications. Springer-Verlag (ISBN 978-0387968889).
ISO, 2006a. Environmental Management — Life Cycle Assessment — Principles and Framework (ISO 14040:2006a). International Standards Organization.
ISO, 2006b. Environmental Management — Life cycle Assessment — Requirements and Guidelines (ISO 14044:2006b). International Organisation for Standardisation.
ISO, 2017. Buildings and Constructed Assets — Service Life Planning — Part 5: Life-cycle Costing (ISO 15686–5:2017). International Organization for Standardization.
Josa, I., Borrion, A., 2025. Rebuilding or retrofitting? An assessment of social impacts using social life cycle assessment. Environ. Impact Assess. Rev. 112, 107794. https://doi.org/10.1016/j.eiar.2024.107794.
Lehne, J., Preston, F., 2018. Making Concrete Change – Innovation in Low-Carbon Cement and Concrete. The Royal Institute of International Affairs, ISBN 978-1784132729.
Madanchian, M., Taherdoost, H., 2023. A comprehensive guide to the TOPSIS method for multi-criteria decision making. Sustain. Soc. Dev. 1 (1), 2220. https://doi.org/10.54517/ssd.v1i1.2220.
McKinsey & Company, 2023. Global Energy Perspective 2023. Executive Summary. https://safety4sea.com/wp-content/uploads/2023/11/McKinsey-Sustainability-%E2%80%93-Global-Energy-Perspective-2023_11.pdf.
Ministry of Public Works, 2008. Structural Concrete Instruction (EHE-08). Government of Spain. https://www.transportes.gob.es/recursos_mfom/1820100.pdf.
Ministry of Transport, Mobility and Urban Agenda, 2021. Structural Code: Royal Decree 470/2021, of June 29. Government of Spain. https://www.boe.es/eli/es/rd/2021/06/29/470/dof/spa/pdf.
Mistry, M., Koffler, C., Wong, S., 2016. LCA and LCC of the world's longest pier: a case study on nickel-containing stainless steel rebar. Int. J. Life Cycle Assess. 21 (11), 1637–1644. https://doi.org/10.1007/s11367-016-1080-2.
Moreno, E.I., Solís, R.G., López, L., 2005. Carbonation-induced Corrosion in Urban Concrete Structures. CORROSION/2005, Paper No. 263. NACE International, Houston, TX.
Navarro, I.J., Yepes, V., Martí, J.V., 2018. Social life cycle assessment of concrete bridge decks exposed to aggressive environments. Environ. Impact Assess. Rev. 72, 50–63. https://doi.org/10.1016/j.eiar.2018.05.003.
Navarro, I.J., Martí, J.V., Yepes, V., 2019. Reliability-based maintenance optimization of corrosion preventive designs under a life cycle perspective. Environ. Impact Assess. Rev. 74, 23–34. https://doi.org/10.1016/j.eiar.2018.10.001.
Navarro, I.J., Yepes, V., Martí, J.V., 2020. Sustainability assessment of concrete bridge deck designs in coastal environments using neutrosophic criteria weights. Struct. Infrastruct. Eng. 16 (7), 949–967. https://doi.org/10.1080/15732479.2019.1676791.
Nolan, S., Rossini, M., Knight, N., Nanni, A., 2021. New directions for reinforced concrete coastal structures. J. Infrastruct. Preserv. Resil. 2 (1). https://doi.org/10.1186/s43065-021-00015-4, 2021.
Otárola, K., Iannacone, L., Gentile, R., Galasso, C., 2024. Multi-hazard life-cycle consequence analysis of deteriorating engineering systems. Struct. Saf. 111, 102515. https://doi.org/10.1016/j.strusafe.2024.102515.
Patrisia, Y., Law, D.W., Gunasekara, C., Wardhono, A., 2022. Life cycle assessment of alkali-activated concretes under marine exposure in an Australian context. Environ. Impact Assess. Rev. 96, 106813. https://doi.org/10.1016/j.eiar.2022.106813.
Rincon, L.F., Moscoso, Y.M., Hamami, A.E.A., Matos, J.C., Bastidas-Arteaga, E., 2024. Degradation models and maintenance strategies for reinforced concrete structures in coastal environments under climate change: a review. Buildings 14 (3), 562. https://doi.org/10.3390/buildings14030562.
Rodrigues, R., Gaboreau, S., Gance, J., Ignatiadis, I., Betelu, S., 2021. Reinforced concrete structures: a review of corrosion mechanisms and advances in electrical methods for corrosion monitoring. Construct. Build Mater. 269, 121240. https://doi.org/10.1016/j.conbuildmat.2020.121240.
Sánchez-Garrido, A.J., Navarro, I.J., Yepes, V., 2021. Neutrosophic multi-criteria evaluation of sustainable alternatives for the structure of single-family homes. Environ. Impact Assess. Rev. 89, 106572. https://doi.org/10.1016/j.eiar.2021.106572.
Sánchez-Garrido, A.J., Navarro, I.J., García, J., Yepes, V., 2023. A systematic literature review on modern methods of construction in building: an integrated approach using machine learning. J. Build. Eng. 73, 106725. https://doi.org/10.1016/j.jobe.2023.106725.
Sánchez-Garrido, A.J., Yepes-Bellver, L., Saiz, D., Yepes, V., 2024a. Project engineering in modern methods of construction: the case of buildings with lightened flat slabs with multiaxial concrete shapers. In: Proceedings of the 28th International Congress on Project Management and Engineering (CIDIP 2024). Asociación Española de Dirección e Ingeniería de Proyectos (AEIPRO), pp. 392–406. https://doi.org/10.61547/2402009.
Sánchez-Garrido, A.J., Navarro, I.J., Yepes, V., 2024b. Sustainable preventive maintenance of MMC-based concrete building structures in a harsh environment. J. Build. Eng. 95, 110155. https://doi.org/10.1016/j.jobe.2024.110155.
Schnellenbach-Held, M., Pfeffer, K., 2002. Punching behavior of biaxial hollow slabs. Cem. Concr. Compos. 24 (6), 551–556. https://doi.org/10.1016/S0958-9465(01)00071-3.
Schoenmaker, D., Schramade, W., 2024. Which discount rate for sustainability? J. Sustain. Finance Account. 3, 100010. https://doi.org/10.1016/j.josfa.2024.100010.
Schöggl, J.-P., Stumpf, L., Baumgartner, R.J., 2020. The narrative of sustainability and circular economy - a longitudinal review of two decades of research. Resour. Conserv. Recycl. 163, 105073. https://doi.org/10.1016/j.resconrec.2020.105073.
Sharma, V.A., Shree, V., Nautiyal, H., 2012. Life cycle environmental assessment of an educational building in northern India: a case study. Sustain. Cities Soc. 4, 22–28. https://doi.org/10.1016/j.scs.2012.03.002.
Sodenkamp, M.A., Tavana, M., Di Caprio, D., 2018. An aggregation method for solving group multi-criteria decision-making problems with single-valued neutrosophic sets. Appl. Soft Comput. 71, 715–727. https://doi.org/10.1016/j.asoc.2018.07.020.
Stenström, C., Norrbin, P., Parida, A., Kumar, U., 2016. Preventive and corrective maintenance – cost comparison and cost–benefit analysis. Struct. Infrastruct. Eng. 12, 603–617. https://doi.org/10.1080/15732479.2015.1032983.
Tuutti, K., 1982. Corrosion of steel in concrete (CBI report no. 4-82). Swedish cement and concrete institute (CBI). https://lucris.lub.lu.se/ws/portalfiles/portal/4709458/3173290.pdf.
UNEP/SETAC, 2009. Guidelines for Social Life Cycle Assessment of Products. United Nations Environment Program. https://www.lifecycleinitiative.org/wp-content/uploads/2012/12/2009%20-%20Guidelines%20for%20sLCA%20-%20EN.pdf.
UNEP/SETAC, 2013. Methodological Sheets for the Subcategories of Social Life Cycle Assessment (S-LCA). https://www.lifecycleinitiative.org/wp-content/uploads/2013/11/S-LCA_methodological_sheets_11.11.13.pdf.
Valderrama, F.G., 2009. Planning of works from top to bottom. In: V Technical and Technological Convention of Technical Architecture (CONTART 09), Albacete, Spain, March 25-27th. https://www.rib-software.es/pdf/Art%C3%ADculos/Planificaci%C3%B3n-de-obras-de-arriba-a-abajo-BIA-271-feb-2012.pdf.
Villalba, P., Sánchez-Garrido, A., Yepes, V., 2024. A review of multi-criteria decision-making methods for building assessment, selection, and retrofit. J. Civil Eng. Manag. 30 (5), 465–480. https://doi.org/10.3846/jcem.2024.21621.
Wittocx, L., Buyle, M., Audenaert, A., Seuntjens, O., Renne, N., Craeye, B., 2022. Revamping corrosion damaged reinforced concrete balconies: life cycle assessment and life cycle cost of life-extending repair methods. J. Build. Eng. 52, 104436. https://doi.org/10.1016/j.jobe.2022.104436.
Yang, D.Y., Frangopol, D.M., 2019. Life-cycle management of deteriorating civil infrastructure considering resilience to lifetime hazards: a general approach based on renewal-reward processes. Reliabil. Eng. Syst. Saf. 183, 197–212. https://doi.org/10.1016/j.ress.2018.11.016.
Yepes-Bellver, L., Brun-Izquierdo, A., Alcalá, J., Yepes, V., 2024. Artificial neural network and kriging surrogate model for embodied energy optimization of prestressed slab bridges. Sustainability 16 (19), 8450. https://doi.org/10.3390/su16198450.
Zavadskas, E.K., Antuchevičienė, J., Kaplinski, O., 2016. Multi-criteria decision making in civil engineering. Part II – applications. Eng. Struct. Technol. 7 (4), 151–167. https://doi.org/10.3846/2029882X.2016.1139664.
Zhang, Y., Kim, C.-W., Tee, K.F., Lam, J.S.L., 2017. Optimal sustainable life cycle maintenance strategies for port infrastructures. J. Clean. Prod. 142, 1693–1709. https://doi.org/10.1016/j.jclepro.2016.11.120.
Zhou, Z., Zhou, J., Alcalá, J., Yepes, V., 2024. Thermal coupling optimization of bridge environmental impact under natural conditions. Environ. Impact Assess. Rev. 104, 107316. https://doi.org/10.1016/j.eiar.2023.107316.
Zhu, X., Meng, X., Zhang, M., 2021. Application of multiple criteria decision making methods in construction: a systematic literature review. J. Civ. Eng. Manag. 27 (6), 372–403. https://doi.org/10.3846/jcem.2021.15260.